

SPE 21221

Seventh SPE Comparative Solution Project: Modelling of Horizontal Wells in Reservoir Simulation

by Long Nghiem, David A. Collins, and Ravi Sharma, *Computer Modelling Group*

SPE Members

Copyright 1991, Society of Petroleum Engineers, Inc.

This paper was prepared for presentation at the 11th SPE Symposium on Reservoir Simulation held in Anaheim, California, February 17-20, 1991.

This paper was selected for presentation by an SPE Program Committee following review of information contained in an abstract submitted by the author(s). Contents of the paper, as presented, have not been reviewed by the Society of Petroleum Engineers and are subject to correction by the author(s). The material, as presented, does not necessarily reflect any position of the Society of Petroleum Engineers, its officers, or members. Papers presented at SPE meetings are subject to publication review by Editorial Committees of the Society of Petroleum Engineers. Permission to copy is restricted to an abstract of not more than 300 words. Illustrations may not be copied. The abstract should contain conspicuous acknowledgment of where and by whom the paper is presented. Write Publications Manager, SPE, P.O. Box 833836, Richardson, TX 75083-3836 U.S.A. Telex, 730989 SPEDAL.

ABSTRACT

This paper reports the results of comparisons of simulation runs performed by fourteen organizations on a problem involving production from a horizontal well in a reservoir where coning tendencies are important. The effect of well length and rates on the recovery is examined. In addition, the paper also reports the techniques used by the different participants to calculate the inflow into the horizontal well and the wellbore hydraulics.

A variety of methods was used by the participants to model the inflow into the horizontal wells ranging from the use of productivity indices to grid refinement. A multitude of techniques was also used to calculate wellbore hydraulics while a few participants selected to represent the wellbore by a constant-pressure line sink.

All participants consistently predict a decrease in the coning behavior with an increase in well length. However, variations in the predictions were observed. Although the modelling methods from different participants can be grouped into different categories, no trend in the predicted results, according to the methods used, could be observed.

References and figures at end of paper.

INTRODUCTION

Recent interest in horizontal wells has been rapidly accelerating because of improved drilling technology, and the increased efficiency and economy of oil recovery operations. This paper presents a problem which deals with the effect of horizontal well lengths and rates on the recovery and selected results as submitted by the participants, compares various approaches for modelling horizontal wells in reservoir simulation, and discusses any large differences in the submitted results. This paper is the seventh in a series of comparative solution projects (CSP)¹⁻⁶ dealing with different aspects of reservoir simulation.

The objectives of this paper are:

1. To compare predictions from different participants.
2. To compare different approaches for calculating pressure drops in the wellbore. The inclusion of wellbore hydraulics in the simulation is preferable. However, participants can also represent the horizontal wellbore by a constant-pressure line sink.
3. To compare different approaches for calculating productivity indices for a horizontal well. Participants can also use local grid refinement around the horizontal well if they so desire.

In designing the problem, an attempt has been made to have the data as simple as possible while maintaining the practicality of the problem. The hope is that major differences in the simulation results are caused by different approaches for calculating pressure drops and productivity indices.

PROBLEM STATEMENT

The problem deals with oil recovery by bottom water drive in a thin reservoir where coning is important. Black-oil fluid properties and relative permeabilities from the Second SPE CSP² are used. However, reservoir and capillary-pressure data are different from those in the Second CSP.

Table 1 shows the reservoir data. Fluid property data are given in Tables 2 and 3, and relative permeabilities and capillary pressures are reported in Table 4. Initial conditions are also given in Table 1. The initial bubble-point pressure is equal to the gridblock oil pressure in each gridblock.

The reservoir is represented by a 9x9x6 grid system. The gridblock dimensions in the horizontal directions (x and y directions) are shown in Figure 1. The thicknesses in the vertical direction (z direction) are reported in Table 1.

Fluids are produced from a horizontal well drilled in the top layer (Layer 1). The well passes through the gridblock centers and the entire length is open to flow. Two lengths are considered:

- a) L=900 ft: well completed in Gridblocks (1,5,1), I=6,7,8
- b) L=2100 ft: well completed in Gridblocks (1,5,1), I=2,3,...,8

The flow direction in the horizontal well is from left to right in Figure 1. Fluids are removed from the portion of the well in Gridblock (8,5,1) to the surface. The horizontal wellbore has an inside diameter of 4.5 inches and an effective relative roughness of 10^{-3} .

A constant pressure line source is used to simulate the bottom water drive. The line source is completed in Gridblocks (1,5,6), I=1,2,...,9 as shown in Figure 2. Pertinent well data for both the injector and the producer are given in Table 5.

The horizontal well produces at a constant liquid (oil and water) rate. Three rates are considered: 3000

STB/day, 6000 STB/day and 9000 STB/day. The following eight cases are considered:

Case 1a:

L=900 ft
 Liquid rate = 3000 STB/day
 Simulation time = 1500 days
 Reporting interval = 100 days

Case 1b:

Same as in Case 1a but with L=2100 ft

Case 2a:

L=900 ft
 Liquid rate = 6000 STB/day
 Simulation time = 1500 days
 Reporting interval = 100 days

Case 2b:

Same as in Case 2a but with L=2100 ft

Case 3a:

L=900 ft
 Liquid rate = 9000 STB/day
 Simulation time = 1500 days
 Reporting interval = 100 days

Case 3b:

Same as in Case 3a but with L=2100 ft

Case 4a:

Horizontal permeabilities = 3000 md for all blocks
 Vertical permeabilities = 300 md for all blocks
 Horizontal well length L = 900 ft
 Liquid production rate = 9000 STB/day
 Minimum bottom hole pressure of producer = 1500 psia
 Water injection rate into the lower horizontal well = 6000 STB/day
 Well index I_{we} for injector in each gridblock = 2.16×10^5 md.ft
 Simulation time = 1500 days
 Reporting interval = 100 days

Case 4b:

Same as in Case 4a but with L = 2100 ft

Cases 4a and 4b differ from the previous cases (Case 1a, 1b, 2a, 2b, 3a, and 3b) in the specification of reservoir permeabilities (Table 1) and in the injector constraint (Table 5). In the six previous cases, the permeabilities are ten times smaller and the injector operates at a bottom-hole pressure constraint of 3700 psia whereas a constant injection rate is maintained for Cases 4a and 4b.

Cases 1 to 3 examine the effect of rates and well lengths on the recovery. Since pressure is maintained, very little free gas is produced. In Case 4, the voidage replacement ratio is less than unity. A substantial amount of gas comes out of solution and is produced with the liquids. Table 6 summarizes the lengths of the producer and the injector/production schemes for the eight cases.

DESCRIPTION OF THE RESERVOIR SIMULATORS

This section describes the reservoir simulators used by the participants. The handling of wellbore hydraulics and of the inflow into the horizontal well are highlighted. Fourteen organizations participated in the Comparative Solution Project. The names and addresses of the participants are listed in Appendix A. Because of space limitations, the write-ups provided by the participants were condensed when required, with retention of the essential features.

ARTEP (Research association of Institut Français du Pétrole, Elf Aquitaine, Total-CFP and Gaz de France)

Sigma-Core, the ARTEP industrial simulator (presently jointly maintained and developed by Franlab) was used for the test examples of the present Project. Sigma-Core is a three-phase, three-dimensional black-oil and compositional model. Several different choices of space and time discretization techniques and matrix solvers are available.

In the runs for this CSP, a fully implicit, five-point difference scheme with upstream mobilities was used. The sparse linear equations were solved by D4 Gaussian elimination. The productivity indices were calculated by matching semi-analytical results (constant-pressure solution line source in a box shaped reservoir with one constant pressure boundary and three no-flux boundaries). The match consisted in reproducing the difference of pressure between the constant pressure boundary and the well and the repartition of well rates along the wellbore. Results are very close to those using Peaceman's formula¹⁴

with a circular permutation of the axes to account for the horizontal well. The values of the productivity indices in md.ft are:

Cases 1a, 2a and 3a:

$$\begin{array}{ll} I=6,8 & I_{we} = 6.52 \times 10^4 \text{ md.ft} \\ I=7 & I_{we} = 5.90 \times 10^4 \text{ md.ft} \end{array}$$

Cases 1b, 2b and 3b:

$$\begin{array}{ll} I=2,8 & I_{we} = 6.63 \times 10^4 \text{ md.ft} \\ I=3,7 & I_{we} = 5.94 \times 10^4 \text{ md.ft} \\ I=4,5,6 & I_{we} = 5.90 \times 10^4 \text{ md.ft} \end{array}$$

The values for Cases 4a and 4b are ten times the values of Cases 1a and 1b respectively.

A very flexible monitoring scheme of injection/production is available for wells, sectors and fields with several wellbore-hydraulic calculations suited for vertical, slanted or horizontal wells. The coupling between wellbore and reservoir is fully implicit.

The wellbore hydraulics used for the current project was from the Pepite model. Reference 7 outlines the main features of this model which can handle two-phase (liquid and gas) flow in pipes with the modelling of stratified and slug flow patterns and the transition from one pattern to the other. It was assumed that rates were constant between two adjacent centers of perforated gridblocks.

Chevron Oil Field Research Company

A fully implicit black-oil simulator with Cartesian local grid refinement capability⁸ was used. Local grid refinement was used to zoom in on the wellbore and replace it with a row of reservoir cells. Darcy's law, for axial flow in those cells, was replaced by a non-linear relationship between pressure drop and fluid velocity. The relationship was derived using Beggs and Brill's multiphase pipe flow correlation⁹. Relative permeability values were calculated, which ensured that the phase velocities in the wellbore were the same as those computed by the correlation (for wellbore gas saturations between 0 and 10%). These relative permeabilities were used for all cases. Flow from the reservoir to the wellbore was treated as cell to cell flow, eliminating the need for defining a productivity index. Flow out of the wellbore occurred in the last wellbore gridblock. The well bottomhole pressure was the pressure in the cell from which fluid was removed.

The multiphase relationships used for liquid (oil+water) and gas are:

$$k_{rj}(S_j) \left| \frac{dp}{dx} \right|_{mn} = 4.46 \cdot 10^{-5} v_{sj} \mu_j + 6.235 \cdot 10^{-6} \rho_j v_{sj}^2$$

$$j=1,g$$

Here k_{rg} and k_{rl} are analogous to gas and liquid relative permeability functions, and v_{sg} and v_{sl} are superficial phase velocities.

Using Beggs and Brill's correlation for liquid saturations in the range from 0.9 to 1.0, and liquid flow rates from 9,000 to 200 reservoir bbl/day, and assuming distributed flow, a least squares fit gives:

$$k_{rg}(S_g) = S_g^{2.2404}$$

$$k_{rl}(S_l) = S_l^{2.9748}$$

For the 900-ft well, each gridblock in (6-8, 5, 1) is locally refined to 3 x 7 x 5 with $\Delta x = 3 \times 100$ ft, $\Delta y = 17$ ft, 8 ft, 4 ft, 2 ft, 4 ft, 8 ft, 17 ft, $\Delta z = 5$ ft, 4 ft, 2 ft, 4 ft, 5 ft. For the 2100-ft well, each gridblock in (2-7, 5, 1) is locally refined to 1 x 7 x 5 with Δy and Δz given as above; Gridblock (8, 5, 1) was locally refined to 3 x 7 x 5 as in the 900-ft well. For both the 900-ft and 2100-ft case, a 2 ft x 2 ft cell at the center of the refined region in the y-z plane represents the wellbore.

Computer Modelling Group (CMG)

The simulator used is IMEX which is an adaptive implicit, three-phase, black-oil simulator with pseudo-miscible options¹⁰. For this study, the hybrid grid refinement and wellbore frictional pressure and slip options^{11,12} were used.

The hybrid grid option results in curvilinear grid refinement within the Cartesian grid about the horizontal or vertical well. The grid is generated automatically based on the reservoir permeabilities, k_1 , k_2 , perpendicular to the well axis and user input number of subdivisions per gridblock. If $k_1 = k_2$ then a circular grid is created. If $k_1 \neq k_2$ then an elliptical grid is created. This provides an accurate and efficient means for modelling near wellbore phenomena allowing the use of coarser Cartesian grids near the wellbore.

The wellbore frictional pressure drop and slip option models the effects of pressure loss due to friction and liquid holdup in the well tubing within the

formation. This is done by coupling a two phase pipeflow correlation with the simulator in a fashion to allow the same primary variable set within the wellbore as within the simulator. Thus wellbore pressures and insitu saturations and bubble point pressures are calculated within a discretized wellbore. Wellbore insitu saturations and pressures were solved fully implicitly with the multiphase flow correlation coupled in an explicit fashion^{11,12}. This also provides an accurate means to model mixing within the wellbore and hence well backflow and crossflow through the wellbore.

When the above two options are used together, as done for this study, the inner grid is cylindrical in shape with the same dimensions as the wellbore. The well productivity then is calculated by using steady-state theory to calculate elliptical (or radial, depending on permeabilities) gridblock locations¹² and using curvilinear transmissibilities.

For the cases in this comparative solution project each Cartesian grid where the wellbore is located was divided into three in the elliptical direction and four in the hyperbolic direction. Dukler's correlation¹⁷ for multiphase flow in pipes was used in the present study.

ECL Petroleum Technologies (ECL)

Eclipse 100 is a fully-implicit, three-phase, general purpose black-oil simulator with gas condensate options. A series of special extensions to this simulator is available, collectively known as Eclipse 200. Two of these special extensions have been applied to this problem: Local Grid Refinement and Wellbore Friction.

The Local Grid Refinement option allows selected regions of a Cartesian grid to be replaced by finer-detailed local grids. The refined local grids are typically placed around wells that require coning effects to be resolved in more detail. The local grids may be Cartesian, 2-D radial (r,z), or 3-D radial with four sectors. Efficiency is enhanced by solving each local grid individually with its own timesteps and iterations, so that small timesteps can be used when necessary without holding up the progress of the global field simulation.

The Wellbore Friction option models the effects of pressure loss due to friction in the well tubing within the formation. It is primarily intended for use with horizontal wells, in which frictional losses may be significant. Eclipse treats the friction head terms in

each well-block connection as additional strongly-coupled variables, which it solves fully implicitly. The frictional pressure drop over a length L of tubing is

$$\Delta p_f = 2 \cdot f \cdot (L/D) \cdot \rho \cdot v^2$$

where f is the Fanning friction factor which, for turbulent flow in rough pipes, is calculated from Haaland's formula¹³. For multiphase flow, a homogeneous model is used, in which the mixture density and viscosity are the flow-weighted averages of the phase properties.

The well indices are calculated from Peaceman's formula for wells penetrating perpendicularly through the centre of rectangular gridblocks¹⁴.

In Cases 4a and 4b the grid was not refined. In Cases 1 to 3 the grid is refined as described below.

The aspect ratio of the well blocks in the yz -direction is approximately unity when transformed to an isotropic system, so a refinement that kept this aspect ratio was applied. The refinement was applied to the box of gridblocks consisting of the row of blocks containing the production well plus an extra block on either end. This box was refined as follows:

z -direction: 3 layers with $\Delta z = 8$ ft, 4 ft, 8 ft
 y -direction: 3 rows with $\Delta y = 24$ ft, 12 ft, 24 ft
 x -direction: 2 blocks at each end of the refinement box were refined into 4, with equal Δx values. The other blocks were not refined in the x -direction.

The refined blocks containing the production well thus had dimensions: $\Delta x = 300$ ft and 150 ft; $\Delta y = 12$ ft; $\Delta z = 4$ ft.

The well index calculated for each of these blocks was 9.75×10^4 and 4.88×10^4 md.ft. For Cases 4a and 4b where no grid refinement was used, the well indices were 5.194×10^5 md.ft.

Robertson ERC Limited (ERC)

The TIGRESS Reservoir Simulator has been used for this project. TIGRESS (The Integrated Geophysics Reservoir Engineering Software System) is an integrated software system which includes application modules for geophysics, geology, petrophysics, mapping, reservoir engineering, reservoir simulation and economics. It operates in a UNIX and X Windows environment with a database and user interface. The TIGRESS software is being developed by Robertson

ERC Limited with significant financial backing from ARCO British Limited, Enterprise Oil plc, Shell UK Limited and The UK Department of Energy. Because of their previous experience in writing the Pores Black Oil Simulator and Scorpio, a Chemical Flood Simulator, the mathematical aspects of the TIGRESS Reservoir Simulator have been developed by AEA Petroleum Services under contract to the TIGRESS consortium. AEA Petroleum Services also carries out the work for this project.

The simulator is based on a generalized compositional formulation which incorporates IMPES and fully implicit solution techniques¹⁵. Fluid properties can be calculated using either black oil or equation of state compositional models. The non-linear equations are solved by Newton's method. Linear equations are solved either by Line Successive Over Relaxation, or by ORTHOMIN with nested factorization preconditioning. Well block productivity indices are calculated using the method of Peaceman¹⁴, modified to allow for a horizontal well by interchanging the x and z axes. The simulator calculates the pressure drop in the wellbore using a modified version of the Beggs and Brill's correlation proposed by Brown¹⁶.

The calculations for this project used a fully implicit solution method and the ORTHOMIN linear solver. The reported results were obtained using the original $9 \times 9 \times 6$ grid. Some of the cases were repeated using local grid refinement in the central region of the model reservoir, but the results were found to be similar to those with the original grid.

HOT Engineering (HOT)

The test problem was solved with the Multipurpose Reservoir Simulation System SURE. SURE is a general non-isothermal compositional model which is formulated for any number of phases and components while the input data and results remain in well-known black-oil format. The available simulation models, from black oil to compositional, are defined blockwise. The models may therefore be changed with time as well as used simultaneously in one reservoir. The grid-refinement option allows construction of a reasonable grid system focusing on interesting areas. This may also be applied dynamically. Using grid gathering, blocks can be merged in aquifer areas. The dynamic implicitness, which was used for this test, reduces the number of implicit unknowns while providing the same quality as the fully implicit method. Direct Gaussian elimination procedure and an iterative solving method (ORTHOMIN) with incom-

plete factorization are available. The latter one was used for this test.

The calculation of pressure drops in horizontal well sections within SURE is based on the Dukler's correlation¹⁷ and is done explicitly. This is because it meets both our requirements by being sufficiently accurate in comparison to other models, and by having a moderate calculation demand.

This calculation model is based on a wide range of experimental data which supplies the necessary information to correlate the most significant variables in multiphase flow: liquid hold-up and friction factor. The calculations do not include the effect of different flow patterns on pressure losses, thus resulting in a simpler calculation model. The basic equation used in this correlation is the familiar Weisbach's friction loss formula. Dukler proposed a different formula for friction loss which includes mixture properties and liquid hold-up.

The productivity indices are calculated from Peaceman's method¹⁴. This gives a value of 5.19×10^4 md.ft for Cases 1, 2 and 3 and 5.19×10^5 md.ft for Case 4.

Integrated Technologies (INTECH)

The simulator used is the VIP-ENCORE simulator developed originally by the firm J.S. Nolen and Associates (now part of INTECH). VIP-ENCORE is the "black-oil" simulator module of the VIP-EXECUTIVE simulator software system. VIP-ENCORE is a three-phase, three-dimensional, vectorized, fully-implicit (or IMPES) simulator in which internally the hydrocarbon fluids are handled compositionally. Fluid data input can be in the conventional "black-oil" tabular form or as a two- or multi-component system defined by pressure-dependent k-values. The BLITZ matrix solver, also developed originally by J.S. Nolen and Associates, was used in the simulations described herein.

Wellbore hydraulics calculations for the horizontal section are not implemented in VIP-ENCORE. In lieu of that, the horizontal wellbore is simulated by a row of high-transmissibility blocks. The transmissibility used to simulate wellbore flow is that value which allows a match of the pressure drop obtained from a multiphase, horizontal flow calculation¹⁸. Because the pressure drop in the simulated wellbore is from block center to block center, the values reported are for 600 ft and 1800 ft, respectively, rather than the actual

wellbore lengths of 900 ft and 2100 ft. (In all cases investigated the pressure drop is very small - maximum 0.5 psi/100 ft).

Simulation of the wellbore with a row of high-transmissibility gridblocks provides two additional benefits. First, it provides a measure of grid refinement because in the y and z directions there are three blocks rather than one. Second, well productivity is determined by the transmissibilities of the block faces, so no "well index" or similar factor is required for each perforated gridblock. (It is necessary, however, to adjust transmissibilities at the wellbore, as described later).

The eight runs specified for the Seventh CSP were all made using a row of gridblocks for the wellbore. As a result, INTECH's grid dimensions were $9 \times 11 \times 8 = 792$ blocks rather than $9 \times 9 \times 6 = 486$ blocks. The "original" column and row of blocks containing the wellbore ($J=5$, $K=1$) are divided into three columns and three rows respectively with $\Delta y = 29.17$ ft, 1.66 ft, 29.17 ft and $\Delta z = 9.17$ ft, 1.66 ft, 9.17 ft. y- and z-direction spacing of the wellbore blocks is 1.66 ft which is the spacing necessary for the block pressure to equal the steady-state flowing pressure of the well (after Peaceman¹⁹.) All other guidelines (rates, pressures, wellbore lengths) were followed explicitly.

Adjustments (increases) in the y- and z-direction transmissibilities are needed because of the small cross-sectional areas to flow associated with the small Δy and Δz values used to simulate the wellbore along with the relatively long lengths of flow. Nine-point differencing in the vertical plane could help offset this problem, but that is not normally available. INTECH's approach was to use the transmissibilities determined from a finer grid ($9 \times 17 \times 12$) system. The transmissibility of each wellbore block face of the $9 \times 11 \times 8$ grid system was taken as the transmissibility computed at the face between two 1.66 ft blocks in both the y- and z-direction of the $9 \times 17 \times 12$ grid system. Use of these adjusted transmissibilities produced wellbore pressures very close to the method of Babu and Odeh²⁰.

Japan National Oil Corporation (JNOC)

JNOC coupled a fully implicit black-oil model to a model for multi-phase flow in pipes to include wellbore hydraulics in the calculations. The reservoir and wellbore equations are solved sequentially in the coupled model.

In the coupled model, the pressure drop in the wellbore is used instead of the hydraulic head as in the original black-oil model to calculate wellbore flowing pressures at the perforated blocks. The pressure drop was obtained from a previous calculation. Therefore for each horizontal multiblock well, there is one additional unknown, i.e. the well pressure at the last downstream block, just as in the original black-oil model.

The multi-phase pipe flow model calculates the pressure drop in the pipe from data on flow rates, well pressures and well geometry. The calculations are based on the Beggs and Brill correlation⁹ in which the flow regime is determined among six regimes (single-phase liquid, single-phase gas, bubble, stratified, intermittent and annular). The model allows precise calculations by dividing the wellbore element in each gridblock into several subsegments. In the current runs, ten subsegments were used for each wellbore element per gridblock.

The calculations of reservoir and wellbore equations are repeated until the updated well pressure is satisfactorily close to the value from the last calculations. From a practical point of view, iterations between the black-oil model and the wellbore model are required only if there is a drastic change in the production rate.

The productivity indices are calculated using the method of Peaceman¹⁴ for nonsquare gridblocks with anisotropic permeabilities. The calculated values are 5.194×10^4 md.ft for Cases 1, 2 and 3, and 5.194×10^5 md.ft for Case 4.

Marathon Oil Company

Marathon's simulator is fully implicit, three-dimensional and three-phase²¹. It can simulate single- or dual-porosity reservoirs using five-point or nine-point finite difference. For this study, nine-point finite difference in the yz plane (i.e. perpendicular to the horizontal well) was found to give essentially the same results as five-point, therefore the reported results are for five-point. The gas and oil phases are treated by use of a two-component formulation in which the maximum amount of dissolved surface gas in the oil phase and vaporized stocktank oil in the gas phase can be approximated as a function of pressure²².

The horizontal-well pressure drop calculations for this comparative study were obtained using the Mukherjee and Brill correlation²³. The oil, gas and water PVT data were input into an auxiliary program

to calculate tables of pressure drop as a function of oil rate, water-cut and gas-oil ratio using the specified empirical correlation. These tables were input into the simulator. Pressure drop between any two locations in the well is interpolated from the tables using total flow rate from all "upstream" locations in the well. Previous timestep values of flow rate are used to estimate the pressure drop (i.e. calculations are explicit). For this reason, timesteps were limited to be no greater than 10 days. Well connection factors for the producer were calculated using the method of Babu et al²⁴. From the rigorous formulation in Reference 24, a wellbore connection factor for each node was determined to be 5.19×10^4 md.ft for Cases 1, 2 and 3, and 5.19×10^5 md.ft for Case 4.

Phillip's Petroleum Company

Phillip's simulator is a general purpose three-dimensional, three-phase reservoir model that can be used to simulate vertical, inclined and horizontal wells. The model uses a fixed or variable degree of implicitness to solve for pressure, water saturation and gas saturation in saturated cells; and pressure, a water saturation and bubble point pressure in undersaturated cells. Results reported in this work were calculated using the fully implicit reservoir and wellbore pressure options. Productivity indices into each horizontal wellbore gridblock are calculated by Peaceman's method¹⁴.

The equivalent gridblock radius proposed by Babu et al²⁴ was compared to Peaceman's expression with good agreement between the two methods. The grid system specified in the problem statement resulted in an equivalent gridblock radius of 5.86 ft and a productivity index of 5.194×10^4 md.ft for Cases 1a through 3b, and a productivity index of 5.194×10^5 md.ft for Cases 4a and 4b. In this model, horizontal wells are treated as either a line source or a line sink, i.e. no wellbore hydraulics are included. Relative permeabilities were calculated using Stone's second method.

Time increment size was controlled by a dual set of constraints. The maximum saturation change per timestep was limited to 0.05, and the maximum time increment size was limited to 0.10 years to minimize time truncation error.

Reservoir Simulation Research Corporation (RSRC)

The simulator used by RSRC is based on a generalized compositional solution algorithm. This algorithm

supports the use of different fluid-property modules within one basic simulator. The algorithm uses a full Newton-Raphson solution technique which, due to fewer iterations per timestep, is more efficient than other commonly used methods. The calculations are structured so that no material-balance errors occur. The black-oil fluid-property option was used to solve the comparative solution problem. A detailed description of the simulator used in this study is presented in Reference 25. The simulator uses a fully implicit treatment of fluid mobilities at production wells and uses an implicitly calculated bottom-hole pressure to allocate well rates between layers for rate-limited wells.

The productivity index for the horizontal producer in this problem is calculated based on Peaceman's method^{14,26} modified to allow for a horizontal well by interchanging the x- and z-axes. Using the formula for interior wells¹⁴, the productivity indices are 5.19×10^4 md.ft for Cases 1, 2 and 3, and 5.19×10^5 md.ft for Case 4. Using the formula for edge wells²⁶, the respective productivity indices are 2.106×10^4 md.ft and 2.106×10^5 md.ft. It was found that the use of either productivity index produces similar results. The formula for edge wells was used in the simulation reported herein.

The pressure drop in the horizontal wellbore was not included in the simulation results reported.

Shell Development Company

The simulator used was the implicit black-oil version of Shell's multipurpose isothermal reservoir simulator. The unknowns solved for in the simulator are the reference phase pressure and the accumulation of Peaceman's formulas for a vertical well¹⁴ and transposing the x and z dependence in the formulas. The value of the productivity indices were 5.194×10^4 md.ft for Cases 1, 2 and 3 and 5.194×10^5 md.ft for Case 4.

The pressure drops within the wellbore are divided into a gravity and a viscous term. The gravity term uses either a no-slip assumption for the average density of a table of average density as a function of the surface flow rates passing through a completion interval. The average elevation of a completion interval can either be set to the gridblock elevation or be specified by the user. The pressure drop due to viscous forces is calculated from tables of pressure drop per unit length as a function of the surface flow rates flowing through a particular interval. The pipe length between two adjacent completion intervals must

be specified by the user. Although the tabular approach allows for a wide range of pressure drop correlations to be used by the simulator and hence requires an outside program to generate the input data, the Dukler's correlation¹⁷ can be used within the simulator to generate the tables.

Stanford University

The simulator used is a three-dimensional, three-phase research simulator with local grid refinement, hybrid grid and domain decomposition options. The wellbore hydraulics option in the simulator was not used for the runs reported here.

The productivity index was computed by using the analytical solution of the single phase differential equation reported by Babu et al²⁰ and numerical solution of the finite difference equations for single phase flow. In these calculations only the producer was considered. The resulting productivity indices are 5.08×10^4 md.ft for Cases 1, 2 and 3 and 5.08×10^5 md.ft for Case 4.

Calculations were made with maximum timestep size of 100 days for Cases 1, 2 and 3 and that of 50 days for Case 4.

Additional runs with local grid refinement and smaller timesteps were also made. The results however were not significantly different from those reported here.

TDC Reservoir Engineering Services

The TDC simulator, BLOS, is a standard 3-D, 3-phase, 3-component, IMPES, finite-difference based simulator. The model uses a two-point approximation for transmissibilities for enhanced spatial accuracy and a stabilized Runge Kutta time-integration scheme for increased timestep sizes relative to the normal IMPES limitation.

Flow coefficients for the horizontal well were computed using Peaceman's procedure¹⁴. The horizontal well was specified as constant potential, with inflow to each segment being determined by local mobility and pressure drop. We compute a well index of 5.19×10^4 md.ft for Cases 1, 2 and 3 and 5.19×10^5 md.ft for Case 4.

For the stated well parameters, we computed a wellbore pressure drop of approximately 0.011 psi/ft for an oil flow of 9000 STB/day. This would give a

maximum pressure drop of only 3 psi for the link closest to the offtake point. Outer intervals would have lower pressure drops. We, thus, elected to ignore the wellbore hydraulics in the simulations.

SUMMARY

The above descriptions shows a variety of methods for calculating inflow into the well. Participants use either Peaceman's approach¹⁴, Babu et al's approach^{20,24} or their own approach for calculating the productivity indices. These methods all give similar values. Four participants used grid refinement around the well. CHEVRON and ECL used Cartesian local grid refinement while CMG used elliptical local grid refinement. INTECH used finer Cartesian gridblock sizes for the whole row and column of gridblocks containing the wellbore. In CHEVRON, CMG and INTECH's approach, the inflow into the well is calculated from a direct discretization of the flow equations, whereas ECL used Peaceman's formula¹⁴.

Different correlations were also used to calculate the wellbore hydraulics. A few participants selected not to include wellbore hydraulics and represented the wellbore as a line sink with uniform pressure.

Table 7 summarizes the various methods for calculating well inflow and wellbore hydraulics. The symbols that will be used to identify the plots from the different participants are also shown.

RESULTS

Cases 1, 2 and 3

These cases examine the effect of well length and production rates on the recovery. Since pressure is maintained, very little free gas is produced. Refer to Table 6 for a summary description of these cases.

Figures 3 through 8 show the oil rate and cumulative oil produced for the different well lengths and rates. The results show that the use of a longer well reduces the water coning tendencies. Figures 9 through 14 show the corresponding water-oil ratios.

Table 8 shows the values of the cumulative oil produced at 1500 days predicted by the different participants. Some variations in the predicted results are observed. The last two rows of the table show the mean and standard deviation of the predicted cumulative oil.

When the problem was sent out to potential

participants the first time, three-phase relative permeability models were not specified. It was later suggested to participants to use the normalized Stone 2 relative-permeability model²⁷. However, some participants had already completed part of the runs with the Stone 1 three-phase relative-permeability model²⁸. The use of the Stone 1 model should give results similar to the Stone 2 model for Cases 1, 2 and 3 because very little free gas was produced. ECL, HOT and Shell's results for Cases 1, 2 and 3 were obtained with the Stone 1 model, whereas all the other participants used the normalized Stone 2 model.

Figures 15 through 17 shows the cumulative water produced. The variations between the participants are relatively small because the well produced at constant liquid rates with high water-oil ratios. Although not shown here, the amounts of injected water predicted by the participants are very similar. The bottom-hole pressure and pressure drop predicted are almost constant throughout the simulation. The values at 1500 days are shown in Tables 9 and 10 respectively. The results in Table 8 indicate that the standard deviation in the predicted bottom-hole pressure is higher for the shorter well. Table 9 shows a wide variation in the predicted pressure drop. A zero pressure drop corresponds to the use of a uniform-pressure line sink.

Case 4

Cases 4a and 4b were designed to yield a large amount of free gas flowing into the producer. Figures 18 and 19 show the oil rates and cumulative oil produced. There are larger variations in the cumulative oil produced than in Cases 1, 2 and 3. The mean and standard deviations of the cumulative oil produced at 1500 days are given in Table 8. As in the previous cases, there are larger variations for the shorter well.

Figures 20 and 21 show the water production rates. The water rates dropped sharply as the minimum bottom-hole pressure of 1500 psia was reached around 700 to 800 days. The cumulative water production is shown in Figure 22. There is reasonable agreement between different participants. Largest variations occur between 600 and 900 days.

The gas-oil ratios are depicted in Figures 23 and 24, and the cumulative gas production is shown in Figures 25 and 26. Gas production rates peaked around 700 to 800 days and then decreased. As free gas production increased, the decrease in bottom-hole pressure accelerated (Figures 27 and 28). The average

reservoir pressure exhibited a similar behavior. At around 700 to 800 days, the bottom-hole pressure reached its minimum value of 1500 psia. The reservoir pressure was then maintained and free gas production decreased.

Figures 29 and 30 show the predicted pressure drop along the wellbore. The pressure drop increased with increased free gas flow rates. There are sizeable variations in the peak pressure drop predicted. For the 900 ft well, three participants (HOT, INTECH and Marathon) predicted a peak pressure drop of less than 10.5 psia, six participants (ARTEP, CMG, ECL, JNOC and Shell) predicted a pressure drop between 27.6 psia and 32.9 psia whereas ERC predicted a value of 42.5 psia. For the 2100 ft well the predicted pressure drops are larger, with substantial variations among the participants. Chevron predicted substantially higher pressure drops than the values shown in Figures 29 and 30. The variations in pressure drop in Case 4 are much larger than the variations in Cases 1, 2 and 3 because of the large flow rate of free gas in the wellbore.

In Case 4, all participants but Shell used the normalized Stone 2 model for relative permeabilities. Shell used the Stone 1 model for all runs.

Observations

Although the modelling methods from the different participants can be grouped into different categories according to the approaches for calculating well productivity indices and for calculating wellbore hydraulics (pressure drop) (see Table 7), no trend in the predicted results corresponding to the methods used could be observed. Other factors such as truncation errors, convergence criteria, timesteps taken and implicit/explicit formulation could have masked any possible trends in the results.

It is not possible to identify the effect of wellbore hydraulics in the results. A recent study¹² shows that runs with and without wellbore hydraulics may give similar cumulative productions for the cases considered; however, the inclusion of wellbore hydraulics in the calculations yields a substantially different drainage pattern along the wellbore. Thus, information on rates and cumulative production per well element would be required. This information was not requested in the problem statement. The effect of wellbore hydraulics is more pronounced in high-permeability reservoirs than in low-permeability reservoirs. Indeed, the effect depends on the ratio between pressure drop and pressure drawdown, and

increases with this ratio.

Table 11 shows the total number of timesteps and Newtonian iterations from the participants. Runs with the shorter well seemed to require more timesteps and iterations than runs with the longer well for most participants although there were exceptions. This can be attributed to a stronger coning behavior associated with the shorter well which makes the problem more difficult to solve. Participants who used grid refinement may require more timesteps and iterations than would otherwise be required. This is due to small gridblocks used near the well.

Note that participants were requested to provide results at every 100 days. The plots were generated by joining these results by straight lines. Smoother curves could have been obtained if more frequent results were reported.

CONCLUSIONS

This Comparative Solution Project deals with the effect of varying the rate and the length of a horizontal well on the recovery of oil from a reservoir where coning is important. Two salient aspects of modelling a horizontal well were examined, namely 1) the calculation of inflow into the well, and 2) the handling of the wellbore hydraulics.

A variety of methods was used by the participants to address the above aspects. They all consistently predicted a decrease in the coning behavior with an increase in well length.

The calculation of inflow into a horizontal well has been a subject of much research and discussion recently²⁹⁻³³. The variety of methods used by the participants suggests that this is an area of active research. An important aspect to investigate would be the effect of grid spacing on the inflow calculation. In the current problem, the grid spacings of the well block in the y and z direction are respectively 60 ft and 20 ft, which are reasonably small.

The inclusion of wellbore hydraulics in a reservoir simulator has been mentioned in the literature. However, few details were given. In view of the variety of techniques used by the participants, publications discussing in detail the techniques used and their importance in reservoir simulation would certainly be welcome. A comparison of different multiphase flow correlations for horizontal wellbore flow in the context of reservoir simulation would also be desirable.

NOMENCLATURE

D	wellbore inside diameter
f	friction factor
I_{we}	well index
k_{rj}	relative permeability for Phase j
L	wellbore length
p	pressure
S_j	saturation of Phase j
v	velocity
v_{sj}	superficial velocity of Phase j
Δp_f	frictional pressure drop
Δx	grid spacing in x direction
Δy	grid spacing in y direction
Δz	grid spacing in z direction
μ_j	viscosity of Phase j
ρ_j	density of Phase j

Subscripts

l	liquid
g	gas

ACKNOWLEDGEMENTS

We thank all participants in this CSP for providing their results and modelling techniques to this paper. Their time and effort in making the runs and their prompt response to our requests are gratefully acknowledged. We also thank Dr. D. Nathan Meehan of Union Pacific Resources and Professor Khalid Aziz of Stanford University for their helpful comments in the design of the problem for this CSP. We are also indebted to Dr. Stephen H. Leventhal of Shell Development Company for performing the preliminary runs to test and check the data given in the problem description.

REFERENCES

- Odeh, A.S., "Comparison of Solutions to a Three-Dimensional Black-Oil Reservoir Simulation Problem," JPT, Vol. 33, January 1981, pp. 13025.
- Weinstein, H.G., Chappellear, J.E., and Nolen, J.S., "Second Comparative Solution Project: A Three-Phase Coning Study," JPT, Vol. 38, March 1986, pp. 345-353.
- Kenyon, D.E., and Behie, G.A., "Third SPE Comparative Solution Project: Gas Cycling of Retrograde Condensate Reservoirs," JPT, Vol. 39, August 1987, pp. 981-998.
- Aziz, K., Ramesh, A.B., and Woo, P.T., "Fourth SPE Comparative Solution Project: A Comparison of Steam Injection Simulators," JPT, Vol. 39, December 1987, pp. 1576-1584.
- Killough, J., and Kossack, C., "Fifth SPE Comparative Solution Project: Evaluation of Miscible Flood Simulators," paper SPE 16000 presented at the Ninth SPE Symposium on Reservoir Simulation, San Antonio, Texas, February 1-4, 1987.
- Firoozabadi, A., and Thomas, L.K., "Sixth SPE Comparative Solution Project: Dual-Porosity Simulators," JPT, Vol. 42, June 1990, pp. 710-715 and 762-763.
- Lagiere, M., Miniscloux, C., and Roux, A., "Computer Two-Phase Flow Model Predicts Pressure and Temperature Profiles," Oil and Gas J., April 1984.
- Wasserman, M.L., "Local Grid Refinement for Three-Dimensional Simulators," paper SPE 16013 presented at the Ninth SPE Symposium on Reservoir Simulation, San Antonio, Texas, February 1-4, 1987.
- Beggs, J.P., and Brill, J.P., "A Study of Two-Phase Flow in Inclined Pipes," JPT, Vol. 25, May 1973, pp. 607-617.
- Fung, L.S.-K., Collins, D.A., and Nghiem, L., "An Adaptive-Implicit Switching Criterion Based on Numerical Stability Analysis," SPERE, Vol. 4, February 1989, pp. 45-51.
- Collins, D., Nghiem, L., Sharma, R., Li, Y.-K., and Jha, K., "Field-Scale Simulation of Horizontal Wells," paper 90-121 presented at the 1990 CIM/SPE International Technical Meeting, Calgary, Alberta, June 10-13.
- Collins, D.A., Nghiem, L., Sharma, R., Agarwal, R., and Jha, K., "Field-Scale Simulation of Horizontal Wells with Hybrid Grids," paper SPE 21218 presented at the 11th SPE Symposium on Reservoir Simulation, February 17-20, 1991, Anaheim, California.
- Haaland, S.E., Trans. ASME, JFE, Vol. 105, 1983, p. 89.

<p>14. Peaceman, D.W., "Interpretation of Well-Block Pressures in Numerical Reservoir Simulation With Nonsquare Gridblock and Anisotropic Permeability," SPEJ, Vol. 23, June 1983, pp. 531-543.</p> <p>15. Mott, R.E., and Farmer, C.L., "A New Formulation for Generalized Compositional Simulation," Second European Conference on the Mathematics of Oil Recovery, Arles, France, September 11-14, 1990.</p> <p>16. Brown, K.E., "The Technology of Artificial Lift Methods," Petroleum Publishing Company, Tulsa, 1977.</p> <p>17. Dukler, A.E., Wicks, M., and Cleveland, R.G., "Frictional Pressure Drop in Two-Phase Flow: An Approach Through Similarity Analysis," A.I.Ch.E. J., Vol. 10, January 1964, pp. 44-51.</p> <p>18. Baxendell, P.B., "Pipeline Flow of Oil and Gas Mixtures," Proceedings Fourth World Petroleum Congress, Sec. II/E, Paper 4.</p> <p>19. Peaceman, D.W., "Interpretation of Well-Block Pressures in Numerical Reservoir Simulation," SPEJ, Vol. 18, June 1978, pp. 183-194.</p> <p>20. Babu, D.K., and Odeh, A.S., "Productivity of a Horizontal Well," SPERE, Vol. 4, November 1989, pp. 417-421.</p> <p>21. Gilman, J.R., and Kazemi, H., "Improvements in Simulation of Naturally Fractured Reservoirs," SPEJ, Vol. 23, August 1983, pp. 695-707.</p> <p>22. Vestal, C.R., and Shank, G.D., "Practical Techniques in Two-Pseudocomponent Black-Oil Simulation," SPERE, Vol. 4, May 1989, pp. 244-252.</p> <p>23. Mukherjee, H., and Brill, J.P., "Liquid Holdup Correlations for Inclined Two-Phase Flow," JPT, Vol. 35, May 1983, pp. 1003-1008.</p> <p>24. Babu, D.K., Odeh, A.S., Al-Khalifa, A.-J.A., and McCann, R.C., "The Relation Between Wellblock and Wellbore Pressure in Numerical Simulation of Horizontal Wells - General Formulas for Arbitrary Well Locations in Grids," unsolicited paper SPE 20161, October 1989.</p>	<p>25. Young, L.C., "Full Field Compositional Modeling on Vector Processors," paper SPE 17803 presented at the SPE Rocky Mountain Regional Meeting, Casper, Wyoming, May 11-13, 1988.</p> <p>26. Peaceman, D.W., "Interpretation of Well-Block Pressures in Numerical Reservoir Simulation: Part 3 - Off-center and Multiple Wells Within a Wellblock," SPERE, Vol. 5, May 1990, pp. 227-232.</p> <p>27. Aziz, K., and Settari, A., Petroleum Reservoir Simulation, Applied Science Publishers Ltd., 1979, London, p. 36.</p> <p>28. Stone, H.L., "Probability Model for Estimating Three-Phase Relative Permeability," JPT, Vol. 22, February 1970, pp. 214-218.</p> <p>29. Peaceman, D.W., "Discussion of Productivity of a Horizontal Well," SPERE, Vol. 5, May 1990, pp. 252-253.</p> <p>30. Brigham, W.E., "Discussion of Productivity of a Horizontal Well," SPERE, Vol. 5, May 1990, pp. 254-255.</p> <p>31. Babu, D.K., and Odeh, A.S., "Author's Reply to Discussion of Productivity of a Horizontal Well," SPERE, Vol. 5, May 1990, pp. 256.</p> <p>32. Peaceman, D.W., "Further Discussion of Productivity of a Horizontal Well," SPERE, Vol. 5, August 1990, pp. 437-438.</p> <p>33. Babu, D.K., and Odeh, A.S., "Author's Reply to Further Discussion of Productivity of a Horizontal Well," SPERE, Vol. 5, August 1990, pp. 438.</p> <p style="text-align: center;">APPENDIX</p> <p>Participants in the Seventh SPE Comparative Solution Project</p> <p>ARTEP Institut Français du Pétrole B.P. 311 92506 Rueil Malmaison Cedex France Contact: Patrick Lemonnier</p>
--	---

Chevron Oil Field Research Company
1300 Beach Boulevard
P.O. Box 446
La Habra, California 90633-0446
U.S.A.
Contact: M.L. Wasserman

Computer Modelling Group
3512 - 33 Street N.W.
Calgary, Alberta T2L 2A6
Canada
Contact: Long Nghiem

ECL Petroleum Technologies
Highlands Farm, Greys Road
Henley-on-Thames, Oxon RG9 4PS
United Kingdom
Contact: Jon Holmes

Robertson ERC Limited
45 West Street
Marlow, Bucks SL7 2LS
United Kingdom
Contact: M.J. Allmen

HOT Engineering
Roseggerstrasse 15
A-8700 Leoben
Austria
Contact: Ludwig Ems

Integrated Technologies
10205 Westheimer
Houston, Texas 77042
U.S.A.
Contact: A.C. Cames, Jr.

Japan National Oil Corporation
Technology Research Center
1-2-2 Hamada, Chiba City
Chiba 260
Japan
Contact: Takao Nanba

Marathon Oil Company
P.O. Box 269
Littleton, Colorado 80160-0269
U.S.A.
Contact: James R. Gilman

Phillip's Petroleum Company
141 Geoscience Building
Bartlesville, Oklahoma 74004
U.S.A.
Contact: Burt Todd

Reservoir Simulation Research Corporation
2525 East 21st Street, Suite 205
Tulsa, Oklahoma 74114-1747
U.S.A.
Contact: Hemanth Kumar

Shell Development Company
Bellaire Research Center
3737 Bellaire Boulevard
P.O. Box 481
Houston, Texas 77001
U.S.A.
Contact: Stephen H. Leventhal

Stanford University
Department of Petroleum Engineering
Mitchell Building 360
Stanford, California 94305-2220
U.S.A.
Contact: Khalid Aziz

TDC Reservoir Engineering Services
555 S. Camino del Rio, Suite A3
Durango, California 81301
U.S.A.
Contact: Michael R. Todd

Table 1 Reservoir Data and Initial Conditions

Layer	Thickness Δz (ft)	Depth to Center of Layer (ft)	Horizontal Permeability (md)*	Vertical Permeability (md)*	P_{oil} (psia)	S_o	S_w
1(top)	20	3600	300	30	3600	0.711	0.289
2	20	3620	300	30	3608	0.652	0.348
3	20	3640	300	30	3616	0.527	0.473
4	20	3660	300	30	3623	0.351	0.649
5	30	3685	300	30	3633	0.131	0.869
6(bottom)	50	3725	300	30	3650	0.000	1.000

Initial bubble-point pressure = gridblock initial oil pressure

*Permeability values for Cases 1 through 3. Horizontal and vertical permeabilities for Case 4 are 3000 md and 300 md respectively.

Table 2 Fluid Property Data
(From Reference 2)

Pressure (psia)	Saturated Properties				
	Solution GOR R_s (SCF/STB)	Oil FVF B_o (RB/STB)	Gas FVF B_g (RB/SCF)	Oil Viscosity μ_o (cp)	Gas Viscosity μ_g (cp)
400	165	1.0120	0.00590	1.17	0.0130
800	335	1.0255	0.00295	1.14	0.0135
1200	500	1.0380	0.00196	1.11	0.0140
1600	665	1.0510	0.00147	1.08	0.0145
2000	828	1.0630	0.00118	1.06	0.0150
2400	985	1.0750	0.00098	1.03	0.0155
2800	1130	1.0870	0.00084	1.00	0.0160
3200	1270	1.0985	0.00074	0.98	0.0165
3600	1390	1.1100	0.00065	0.95	0.0170
4000	1500	1.1200	0.00059	0.94	0.0175
4400	1600	1.1300	0.00054	0.92	0.0180
4800	1676	1.1400	0.00049	0.91	0.0185
5200	1750	1.1480	0.00045	0.90	0.0190
5600	1810	1.1550	0.00042	0.89	0.0195

Oil compressibility for undersaturated oil (psia ⁻¹)	10 ⁻⁵
Oil viscosity compressibility for undersaturated oil (psia ⁻¹)	0.0
Stock tank oil density, ρ_{oil} (lb _m /ft ³)	45.0
Standard-condition gas density, ρ_{gsc} (lb _m /ft ³)	0.0702
Water compressibility, c_w (psia ⁻¹)	3x10 ⁻⁶
Water formation volume factor at reservoir temperature and atmospheric pressure, B_w^* (RB/STB)	1.0142
Water density at standard conditions, ρ_w^* (lb _m /ft ³)	62.14
Reference pressure for water FVF and densities, p_w^* (psia)	14.7
Water viscosity, μ_w (cp)	0.96

Table 3 Property Equations

- Water FVF

$$B_w = B_w^* [1 - c_w (p_w - p_w^*)]$$
 RB/STB
 - Densities

$$\rho_o = (\rho_{oil} + R_s \rho_{gsc} / 5.6146) / B_o \quad \text{lb}_m/\text{ft}^3$$

$$\rho_g = (\rho_{gsc} / 5.6146) / B_g \quad \text{lb}_m/\text{ft}^3$$

$$\rho_w = \rho_w^* [1 + c_w (p_w - p_w^*)] \quad \text{lb}_m/\text{ft}^3$$
 - Porosities

$$\phi = \phi^* [1 + c_\phi (p_o - p^*)]$$

$$\phi^* = 0.20$$
- Rock compressibility, c_ϕ (psia⁻¹) = 4.0 x 10⁻⁶
- Reference pressure, p^* (psia) = 3600.0
- p_o = oil-phase pressure

Table 4 Relative Permeabilities and Capillary Pressures

Water/Oil Functions			
S_w	k_{rw}	k_{rog}	P_{cow} (psia)
0.22	0.00	1.0000	6.30
0.30	0.07	0.4000	3.60
0.40	0.15	0.1250	2.70
0.50	0.24	0.0649	2.25
0.60	0.33	0.0048	1.80
0.80	0.65	0.0000	0.90
0.90	0.83	0.0000	0.45
1.00	1.00	0.0000	0.00

Gas/Oil Functions			
S_g	k_{rg}	k_{rog}	P_{cgo} (psia)
0.00	0.0000	1.00	0.0
0.04	0.0000	0.60	0.2
0.10	0.0220	0.33	0.5
0.20	0.1000	0.10	1.0
0.30	0.2400	0.02	1.5
0.40	0.3400	0.00	2.0
0.50	0.4200	0.00	2.5
0.60	0.5000	0.00	3.0
0.70	0.8125	0.00	3.5
0.78	1.0000	0.00	3.9

Table 5 Well Data

InjectorsCases 1, 2, and 3Well index I_{we} in each gridblock = 2.16×10^4 md.ft

Bottom hole pressure = 3700 psia

Well rate in each gridblock = $\frac{I_{we}}{B_w \mu_w} \Delta p$ Case 4Well index I_{we} in each gridblock = 2.16×10^5 md.ft

Water injection rate = 6000 STB/day

Producer

Wellbore inside diameter = 4.5 inches

Effective relative roughness of wellbore $(k/D) = 10^{-3}$

Minimum bottomhole pressure = 1500 psia

Length = 900 ft and 2100 ft

Liquid (oil and water) rate = 3000 STB/day, 6000 STB/day and 9000 STB/day

Table 6 Horizontal-Producer Lengths and Production/Injection Schemes

Case	Horizontal-Producer Length (ft)	Liquid Production Rate* (stb/day)	Water Injection Scheme
1a	900	3000	p = 3700 psia
1b	2100	3000	p = 3700 psia
2a	900	6000	p = 3700 psia
2b	2100	6000	p = 3700 psia
3a	900	9000	p = 3700 psia
3b	2100	9000	p = 3700 psia
4a	900	9000	$q_w = 6000$ stb/day
4b	2100	9000	$q_w = 6000$ stb/day

*Minimum bottom-hole pressure = 1500 psia

Table 7 Summary of Methods for Calculating Well Inflow and Wellbore Hydraulics

Participant	Symbol	Well Index	Grid Refinement	Wellbore Hydraulics
ARTEP	■	Own approach		Pepite model ⁷
Chevron	□	Direct discretization	Local Cartesian	Beggs and Brill's correlation ⁹
CMG	●	Direct discretization	Local curvilinear	Dukler's correlation ¹⁷
ECL	○	Peaceman ¹⁴	Local Cartesian	Friction factor from homogeneous flow
ERC	▼	Peaceman ¹⁴		Beggs and Brill's correlation ⁹
HOT	▽	Peaceman ¹⁴		Simplified Dukler's approach ⁹
INTECH	▲	Direct discretization	Cartesian	Reference 18
JNOC	△	Peaceman ¹⁴		Beggs and Brill's correlation ⁹
Marathon	◆	Babu et al ²⁴		Mukherjee and Brill's correlation ²⁴
Phillip's	◇	Peaceman ¹⁴		
RSRC	A	Peaceman ²⁶		
Shell	B	Peaceman ¹⁴		Dukler's correlation ¹⁷
Stanford	C	Babu and Odeh ²⁰		
TDC	D	Peaceman ¹⁴		

Table 8 Cumulative Oil Production in MSTB at 1500 Days

Participants	1a	1b	2a	Cases 2b	3a	3b	4a	4b
ARTEP	747.2	951.7	976.4	1221.0	1096.4	1318.5	740.8	902.8
Chevron	741.0	929.4	958.1	1181.6	1066.0	1274.8	665.3	797.7
CMG	753.6	960.1	983.6	1230.3	1106.1	1330.2	709.0	850.6
ECL	757.2	951.0	1034.2	1251.0	1229.1	1444.8	696.7	827.4
ERC	683.5	870.2	900.3	1106.1	1031.4	1222.3	672.0	788.4
HOT	765.0	961.9	1045.9	1263.7	1247.0	1466.8	714.0	877.6
INTECH	723.3	957.5	949.6	1241.5	1103.2	1414.7	754.4	890.4
JNOC	717.4	951.3	931.6	1245.9	1084.4	1412.7	660.6	843.9
Marathon	722.9	964.3	941.5	1257.1	1096.0	1436.7	781.7	895.8
Phillip's	750.9	956.8	980.5	1227.1	1103.5	1325.0	712.0	859.7
RSRC	678.7	916.7	877.9	1177.8	1017.1	1333.2	620.5	801.5
Shell	749.0	954.8	978.4	1224.6	1100.0	1322.4	733.5	884.1
Stanford	742.0	943.9	968.7	1211.8	1043.7	1305.6	331.0	457.6
TDC	766.2	980.4	989.4	1210.0	1105.0	1279.2	845.4	933.6
Mean	735.6	946.4	965.4	1217.8	1102.1	1349.1	688.4	829.4
Standard Deviation	27.4	26.7	45.2	41.0	64.7	73.5	117.0	115.4

Table 9 Bottom-Hole Pressure in psia at 1500 Days

Participants	1a	1b	2a	2b	3a	3b
ARTEP	3466.76	3575.78	3236.68	3470.49	3002.20	3364.74
Chevron	3464.77	3576.10	3239.19	3464.32	3012.13	3356.08
CMG	3446.32	3558.33	3210.46	3454.76	2970.39	3345.85
ECL	3485.03	3569.71	3326.22	3490.41	3170.46	3412.53
ERC	3439.96	3562.14	3199.89	3453.11	2949.06	3343.41
HOT	3511.65	3582.92	3382.08	3520.19	3256.18	3459.89
INTECH	3530.00	3601.00	3382.00	3541.00	3221.00	3479.00
JNOC	3471.72	3589.29	3251.86	3491.07	3020.84	3405.28
Marathon	3493.24	3593.85	3295.26	3509.80	3085.07	3433.56
Phillip's	3449.40	3572.40	3203.40	3460.20	2953.20	3351.90
RSRC	3567.80	3610.90	3444.10	3575.30	3318.90	3530.30
Shell	3448.75	3571.38	3201.16	3456.91	2948.98	3345.16
Stanford	3454.64	3572.29	3216.69	3464.30	2977.69	3359.93
TDC	3438.21	3544.40	3203.95	3452.69	2959.82	3343.16
Mean	3476.30	3577.18	3270.92	3486.04	3060.42	3395.06
Standard Deviation	37.96	17.45	81.54	37.87	127.79	60.28

Table 10 Total Pressure Drop in Wellbore in psia at 1500 Days

Participants	1a	1b	2a	2b	3a	3b
ARTEP	0.40	0.93	1.46	3.34	3.15	7.25
Chevron	1.03	1.42	3.89	5.41	8.57	11.97
CMG	0.46	0.98	1.70	3.57	3.68	7.73
ECL	0.42	0.95	1.53	3.49	3.33	7.55
ERC	0.33	1.05	1.13	3.50	2.25	7.30
HOT	0.21	0.45	1.10	1.50	1.97	3.06
INTECH	0.60	1.70	1.20	3.50	1.70	5.30
JNOC	0.45	1.05	1.86	4.31	4.14	9.58
Marathon	0.26	0.85	0.92	3.04	1.97	6.53
Phillip's	0.00	0.00	0.00	0.00	0.00	0.00
RSRC	0.00	0.00	0.00	0.00	0.00	0.00
Shell	0.48	1.09	1.69	3.74	3.57	7.77
Stanford	0.00	0.00	0.00	0.00	0.00	0.00
TDC	0.00	0.00	0.00	0.00	0.00	0.00

Table 11 Timesteps and Newtonian Iterations

Participants	1a	1b	2a	2b	3a	3b	4a	4b
ARTEP	39 ^(a)	39	45	39	47	42	50	49
Chevron ^(c)	104 ^(b)	94	120	100	124	107	186	171
	36	21	36	23	37	24	66	45
	84	63	96	78	120	92	247	246
CMG ^(c)	24	23	25	25	25	25	31	33
	58	61	62	76	61	66	135	154
ECL ^(d)	23	21	23	23	23	22	35	34
	55	51	64	56	65	57	102	103
ERC	26	25	24	27	24	25	149	343
	39	38	42	43	51	45	459	943
HOT	17	17	17	17	17	17	102	96
	23	23	27	24	27	26	156	182
INTECH ^(c)	31	31	33	31	34	33	82	72
	92	106	105	104	105	114	392	356
JNOC	22	21	23	22	24	22	48	47
	53	48	57	53	57	53	130	134
Marathon	155	155	161	157	165	157	288	252
	221	192	291	233	346	253	898	961
Phillip's	47	46	47	47	47	47	47	50
	57	50	66	56	70	60	104	101
RSRC	58	36	158	44	182	71	1732	1264
	58	36	161	45	197	72	1733	1264
Shell	42	42	45	43	42	43	55	47
	114	109	123	121	120	125	180	153
Stanford	20	19	22	20	22	21	49	43
	55	44	55	50	60	57	265	116
TDC	318	96	632	272	951	421	901	541
	2093	189	4441	1796	6986	2882	7326	3366

- (a) Total number of timesteps
- (b) Total number of iterations
- (c) Use of grid refinement for all cases
- (d) Use of grid refinement with local timesteps and iterations for all cases except 4a and 4b

Figure 1 Horizontal Producer in Top Layer (K=1)

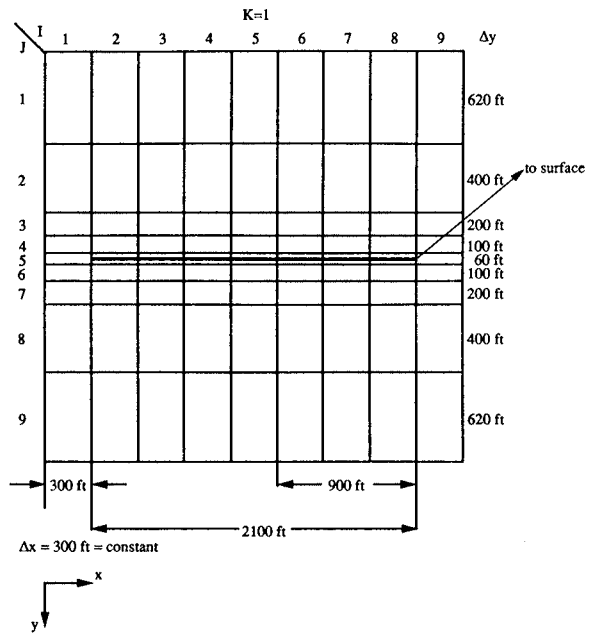


Figure 2 Water Injection in Bottom Layer (K=6)

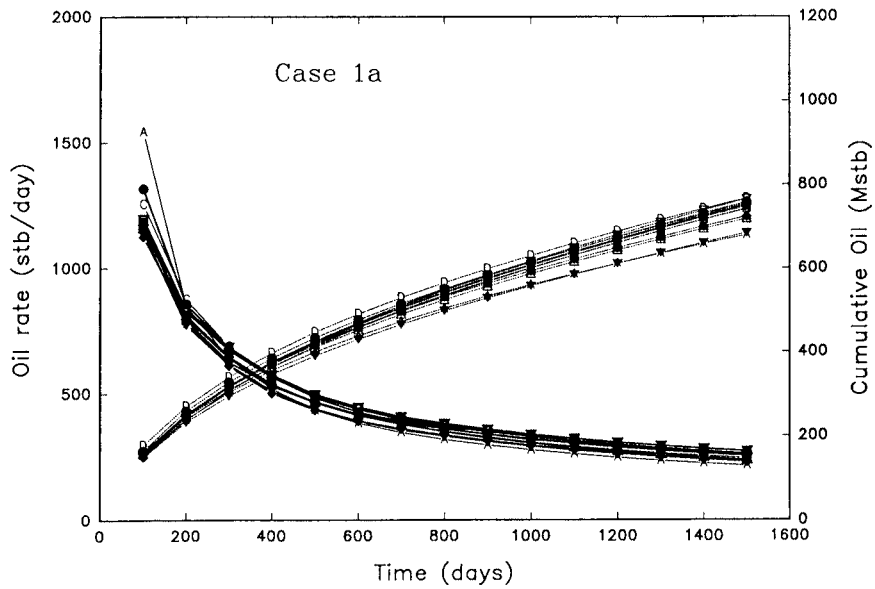
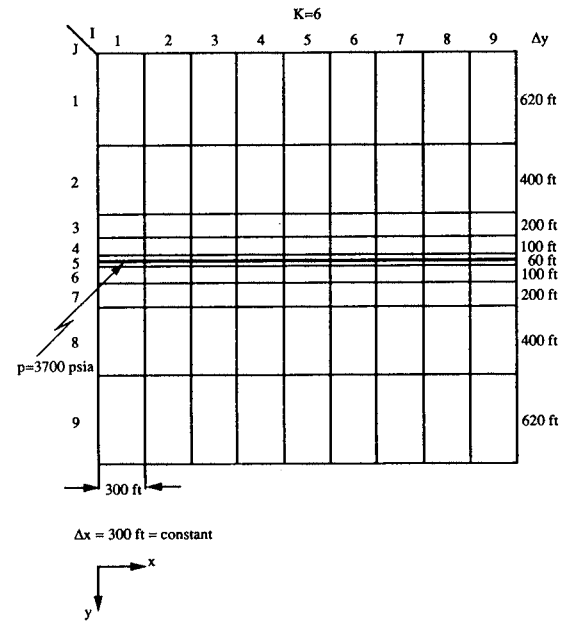


Figure 3: Oil rate (solid) and cumulative oil production (dashed) for Case 1a

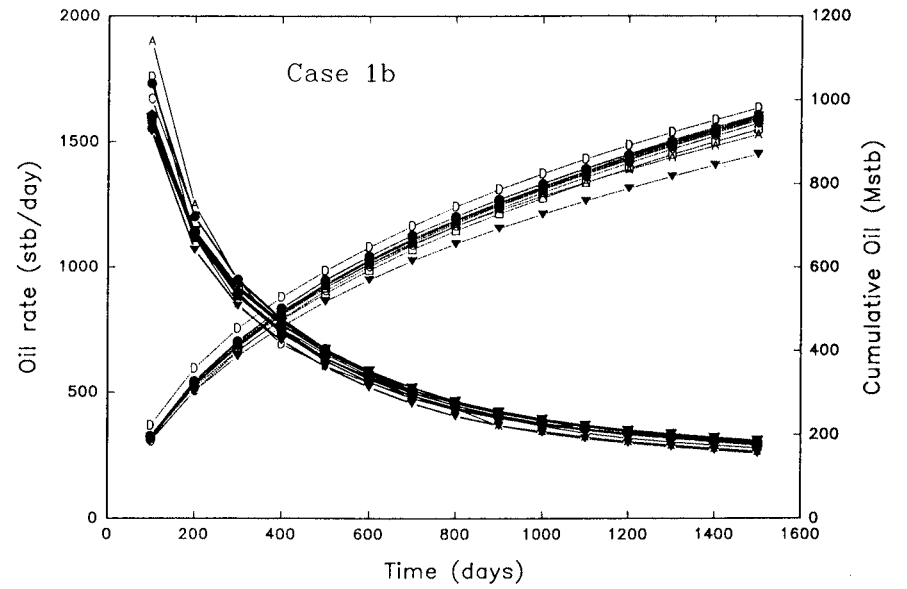


Figure 4: Oil rate (solid) and cumulative oil production (dashed) for Case 1b

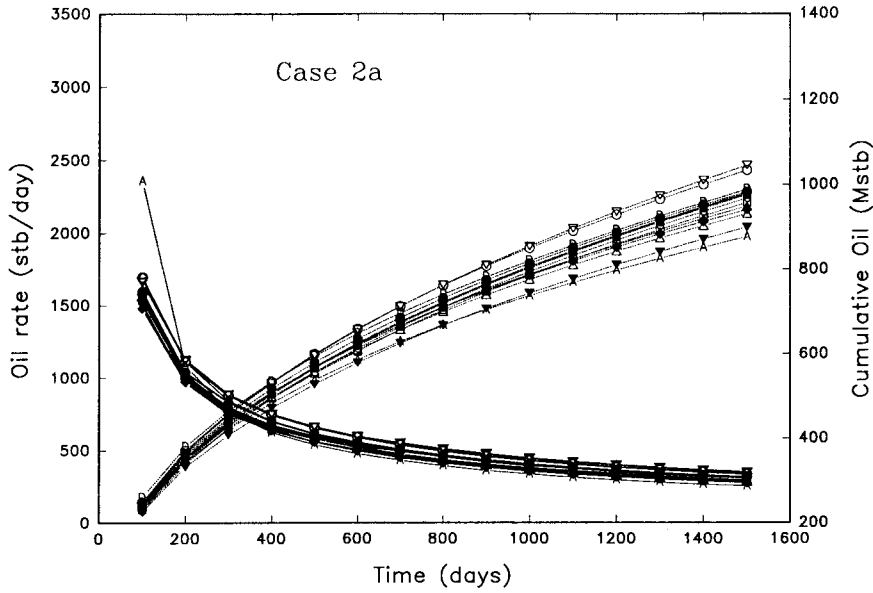


Figure 5: Oil rate (solid) and cumulative oil production (dashed) for Case 2a

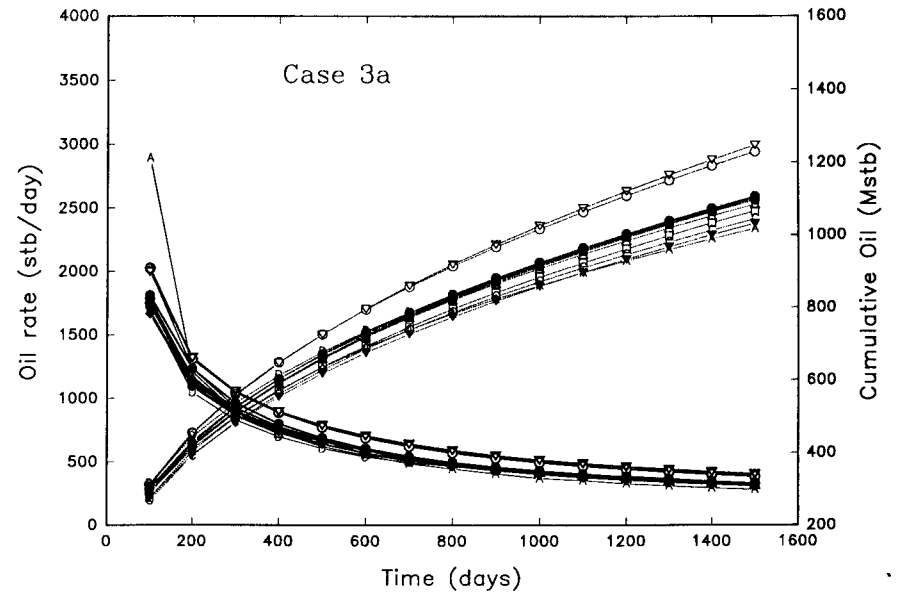


Figure 7: Oil rate (solid) and cumulative oil production (dashed) for Case 3a

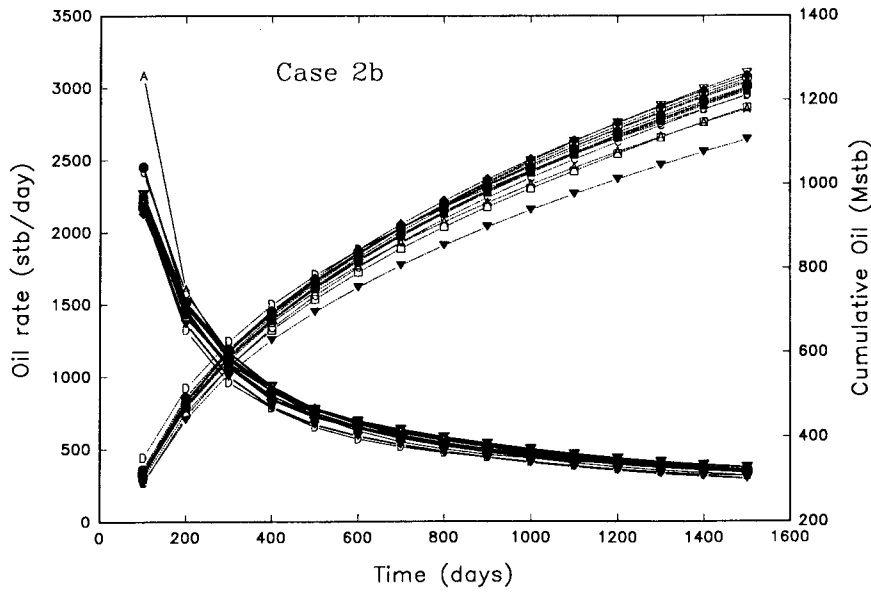


Figure 6: Oil rate (solid) and cumulative oil production (dashed) for Case 2b

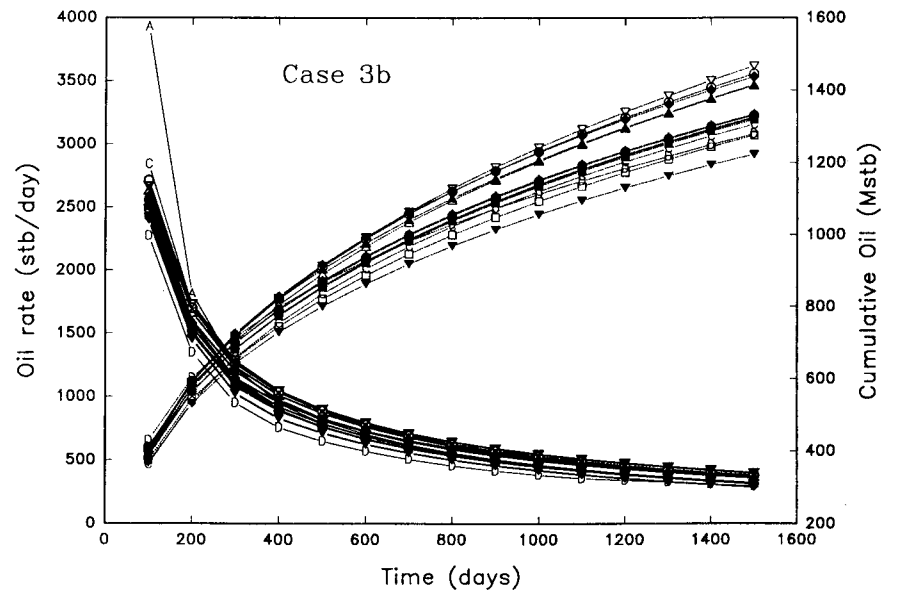


Figure 8: Oil rate (solid) and cumulative oil production (dashed) for Case 3b

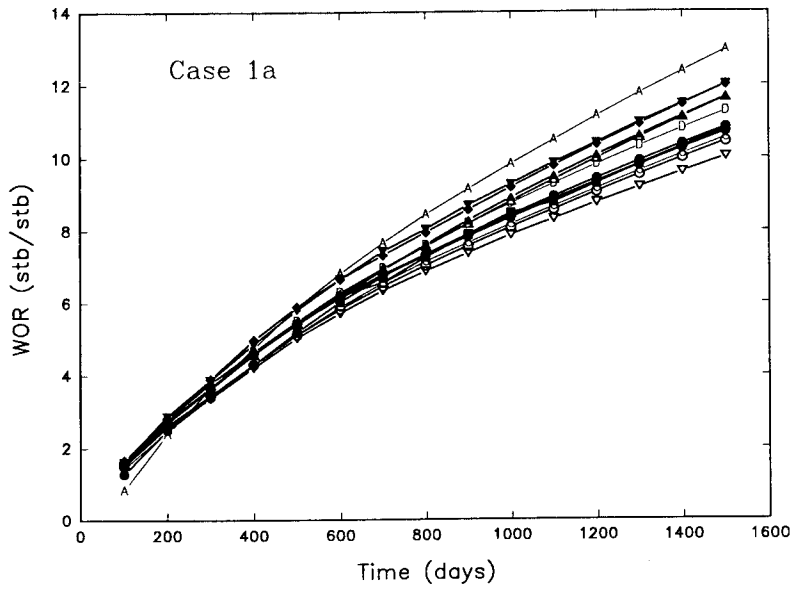


Figure 9: Water-oil ratio for Case 1a

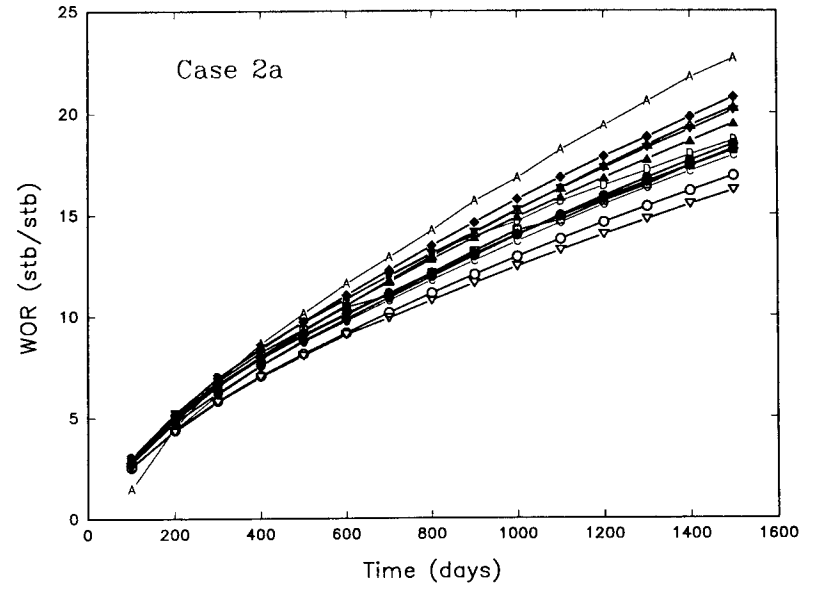


Figure 11: Water-oil ratio for Case 2a

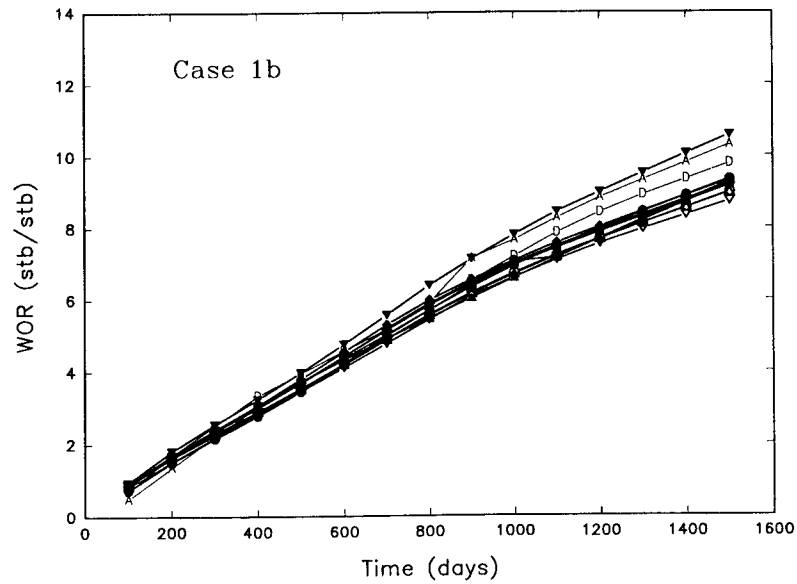


Figure 10: Water-oil ratio for Case 1b

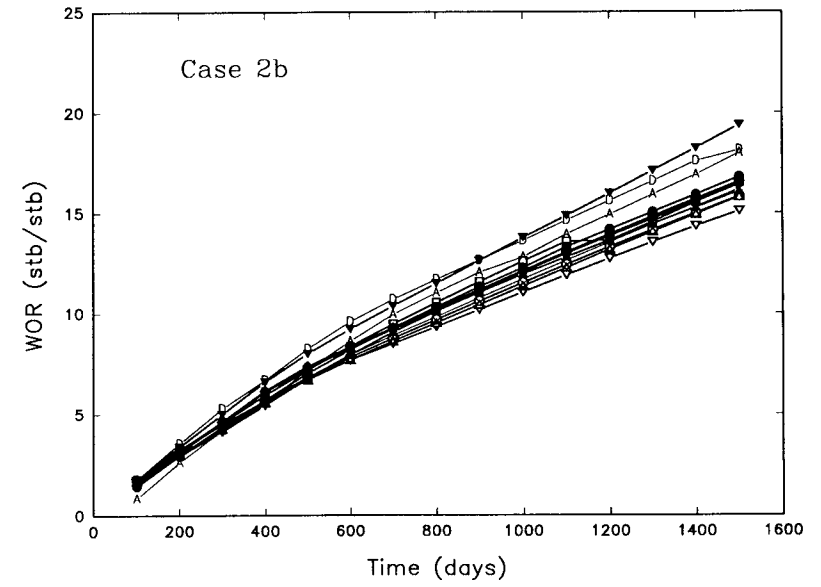


Figure 12: Water-oil ratio for Case 2b

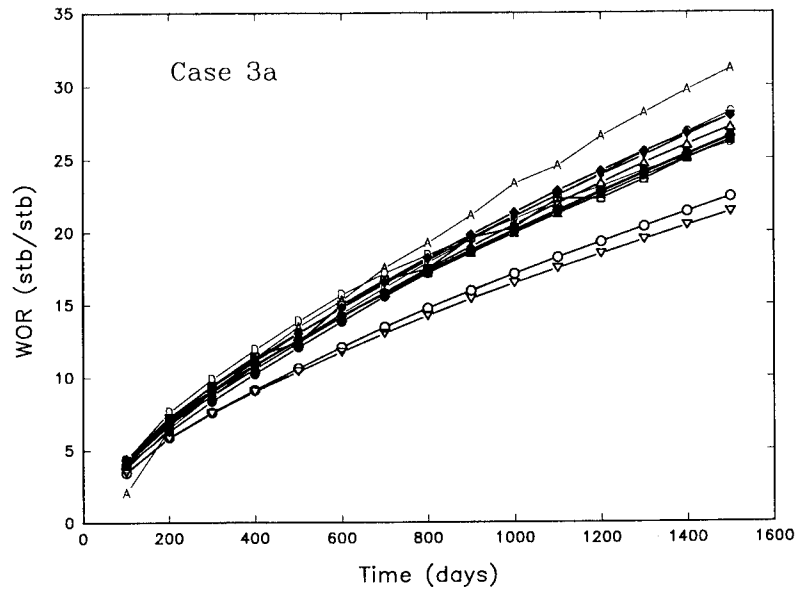


Figure 13: Water-oil ratio for Case 3a

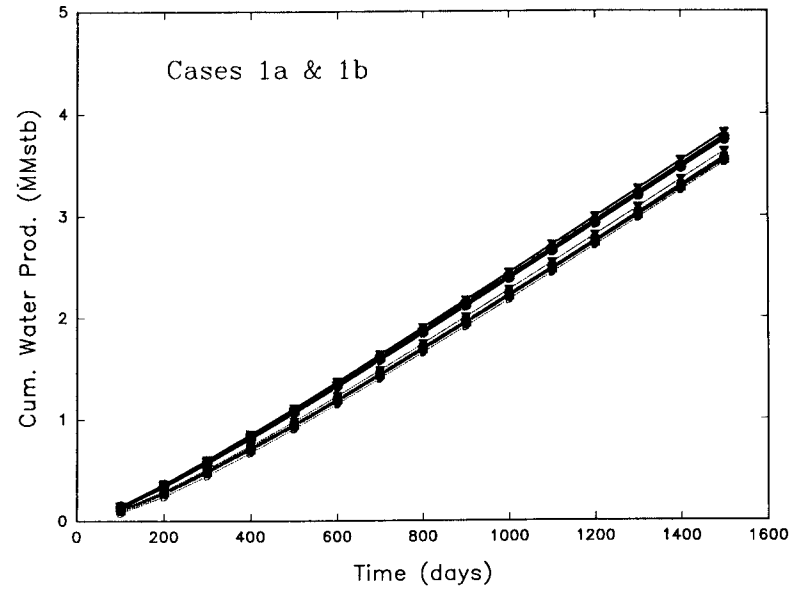


Figure 15: Cumulative water production for Case 1a (solid) and 1b (dashed)

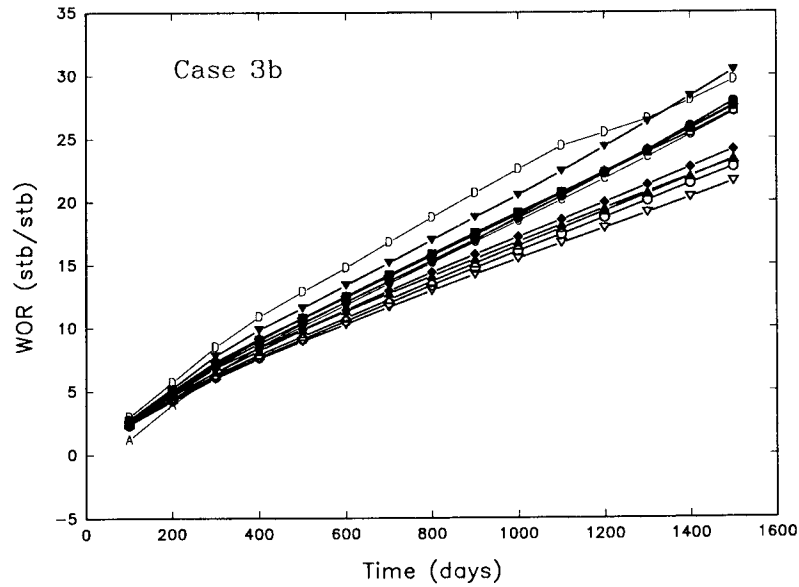


Figure 14: Water-oil ratio for Case 3b

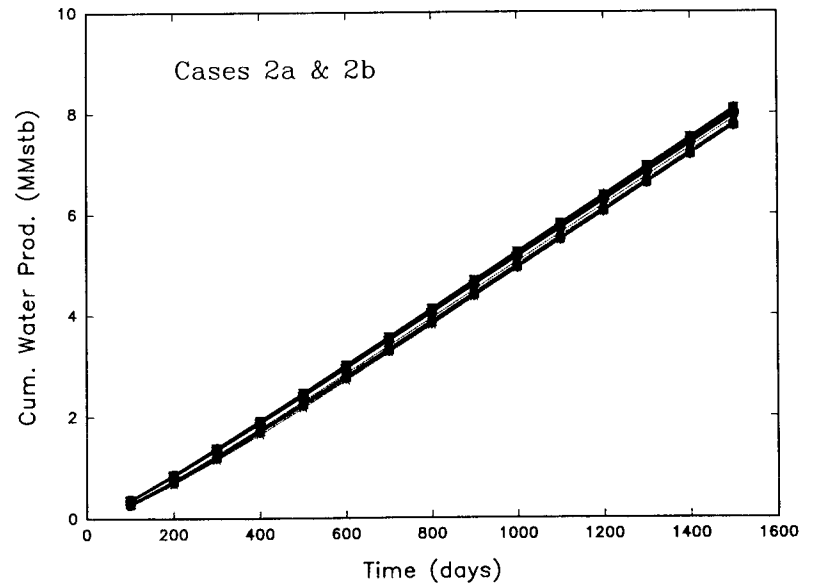


Figure 16: Cumulative water production for Case 2a (solid) and 2b (dashed)

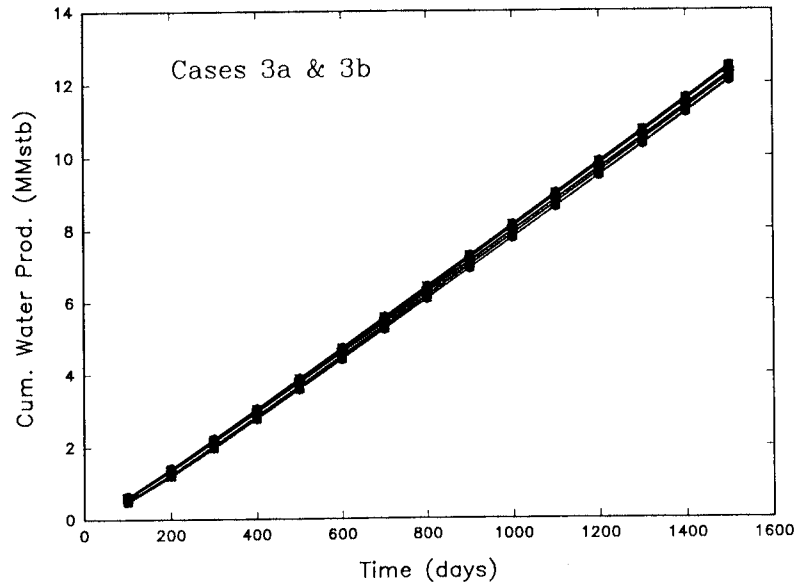


Figure 17: Cumulative water production for Case 3a (solid) and 3b (dashed)

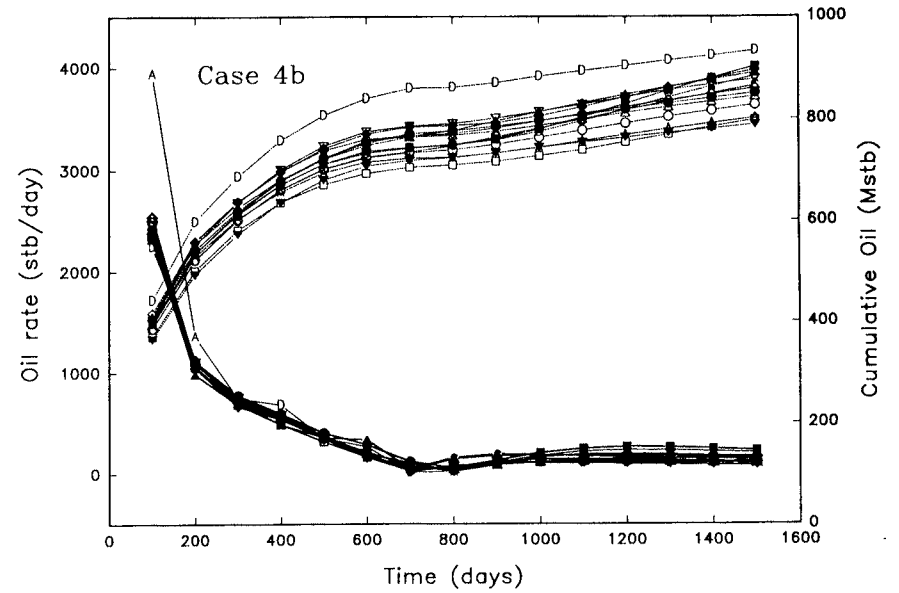


Figure 19: Oil rate (solid) and cumulative oil production (dashed) for Case 4b

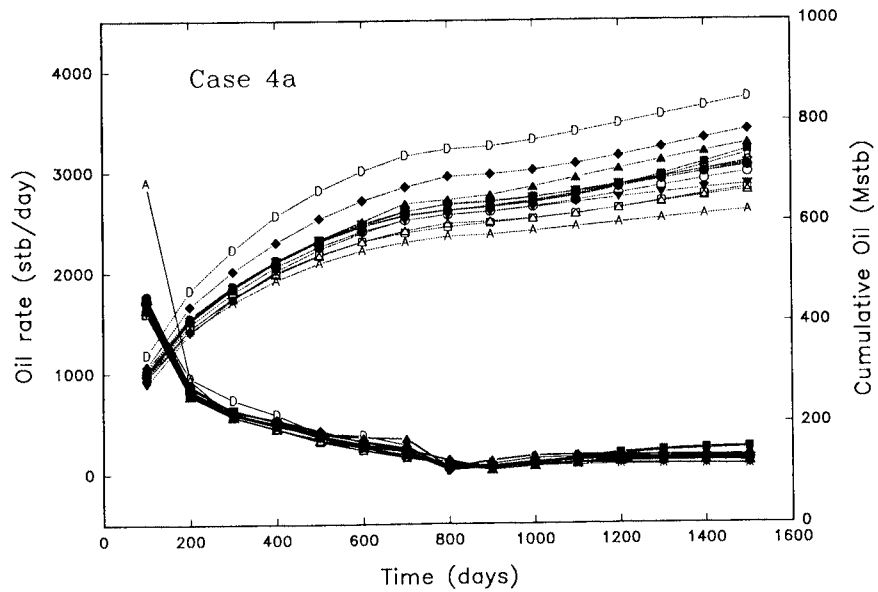


Figure 18: Oil rate (solid) and cumulative oil production (dashed) for Case 4a

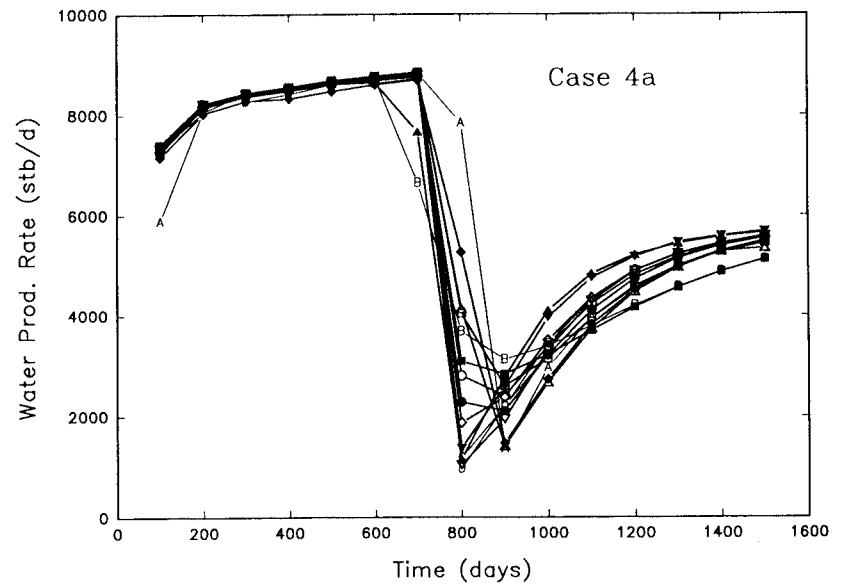


Figure 20: Water production rate for Case 4a

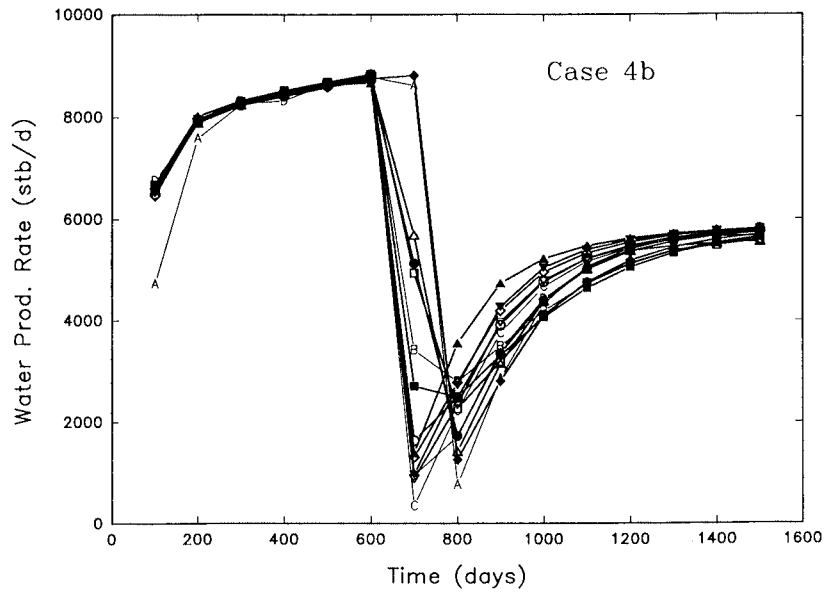


Figure 21: Water production rate for Case 4b

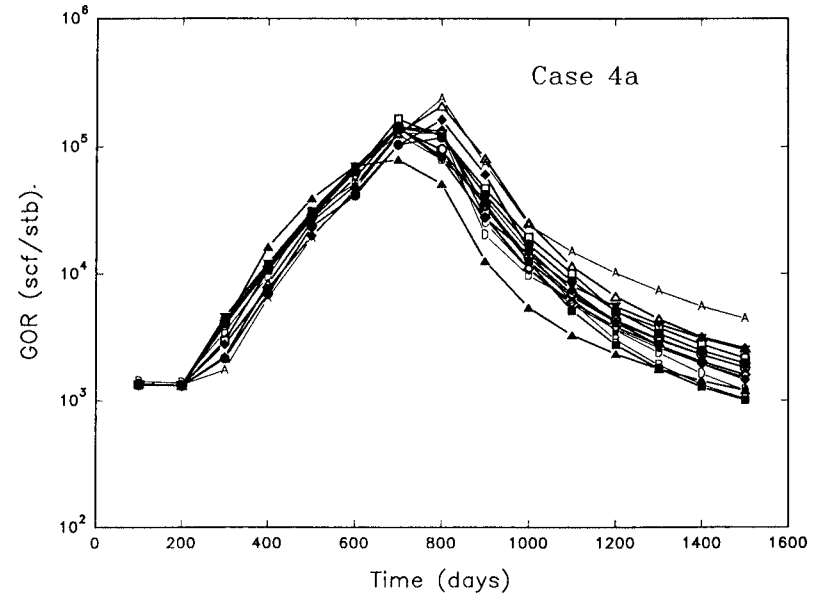


Figure 23: Gas-oil ratio for Case 4a

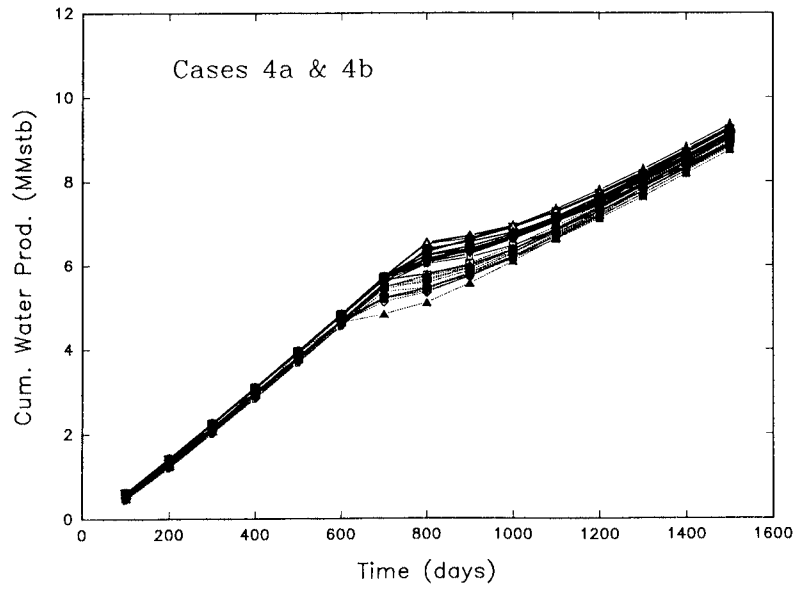


Figure 22: Cumulative water production for Case 4a (solid) and 4b (dashed)

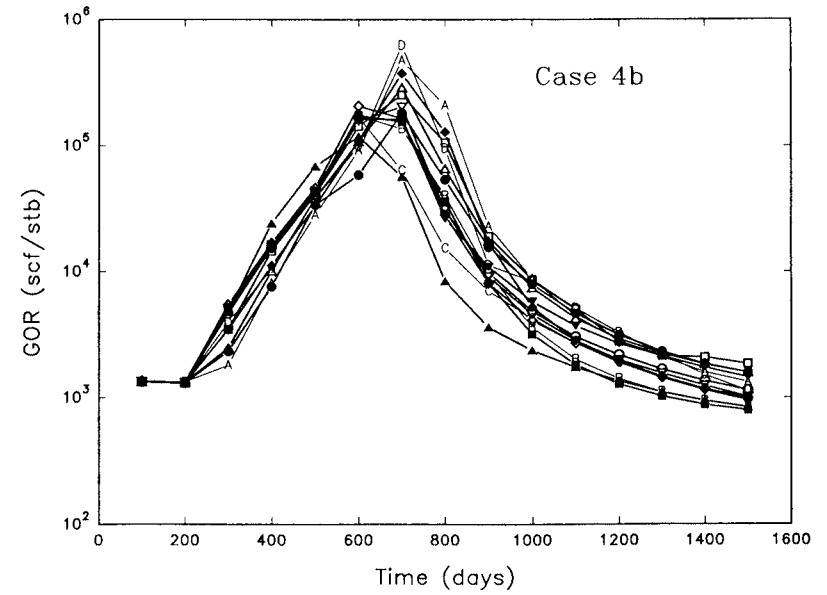


Figure 24: Gas-oil ratio for Case 4b

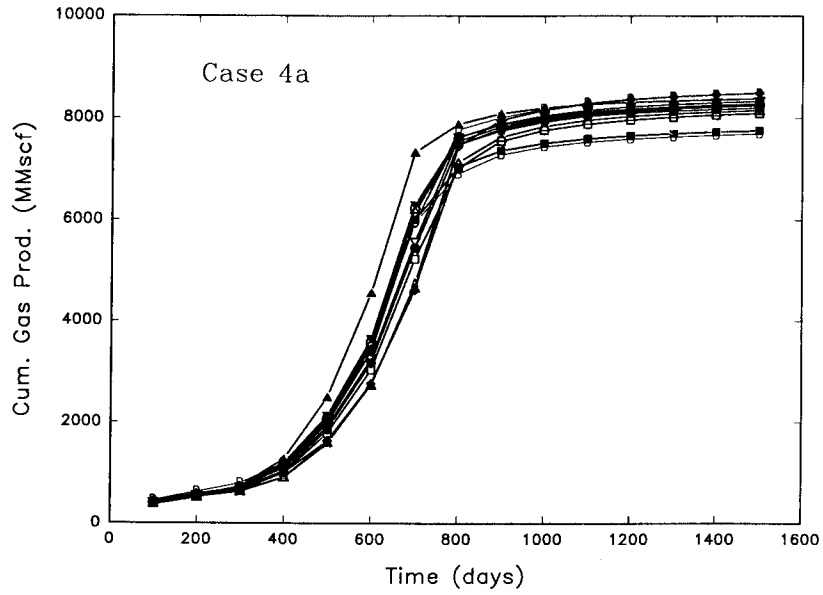


Figure 25: Cumulative gas production for Case 4a

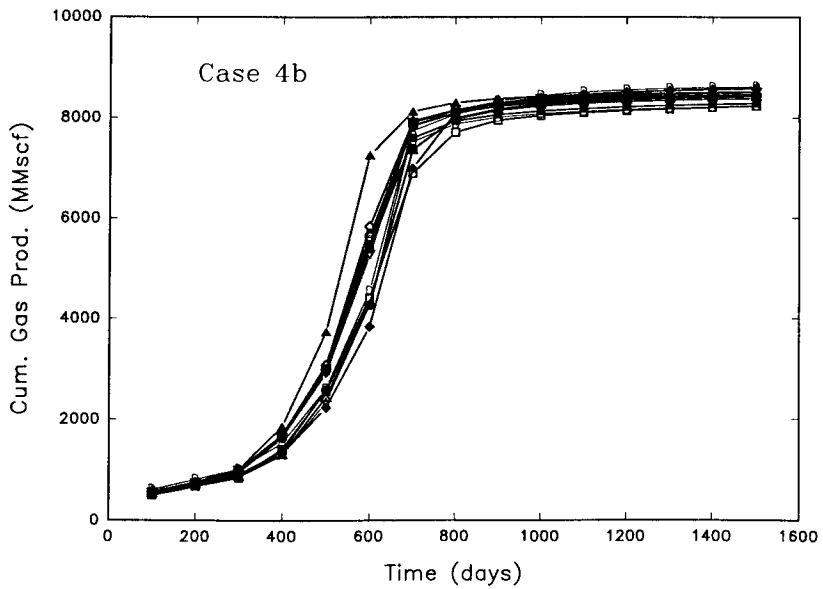


Figure 26: Cumulative gas production for Case 4b

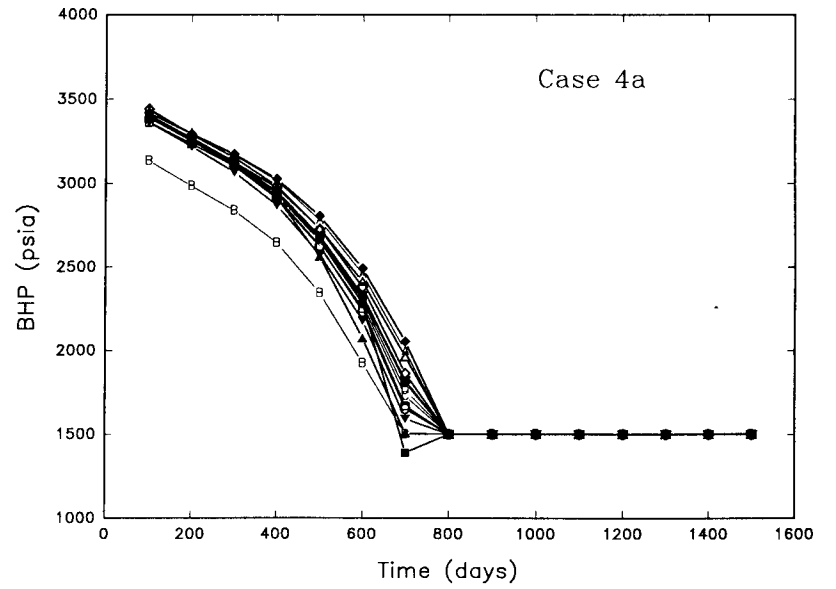


Figure 27: Bottom-hole pressure for Case 4a

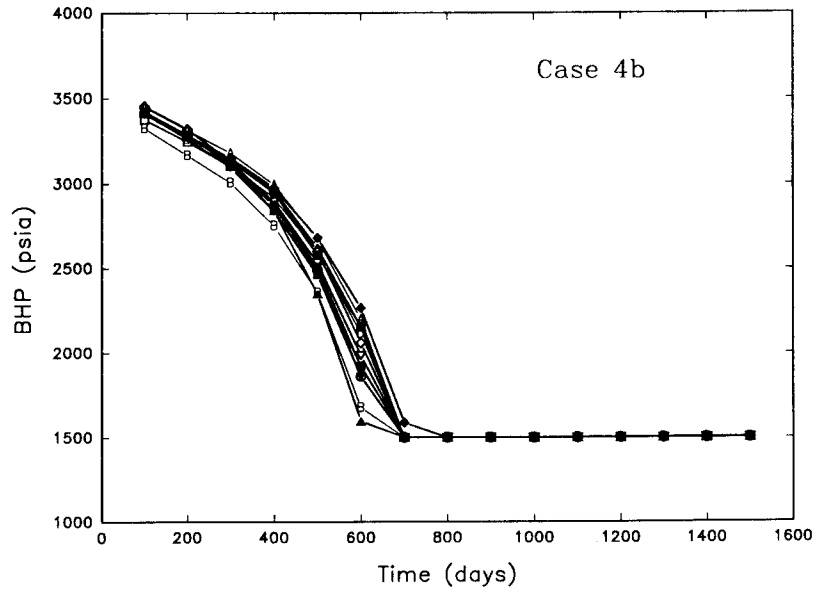


Figure 28: Bottom-hole pressure for Case 4b

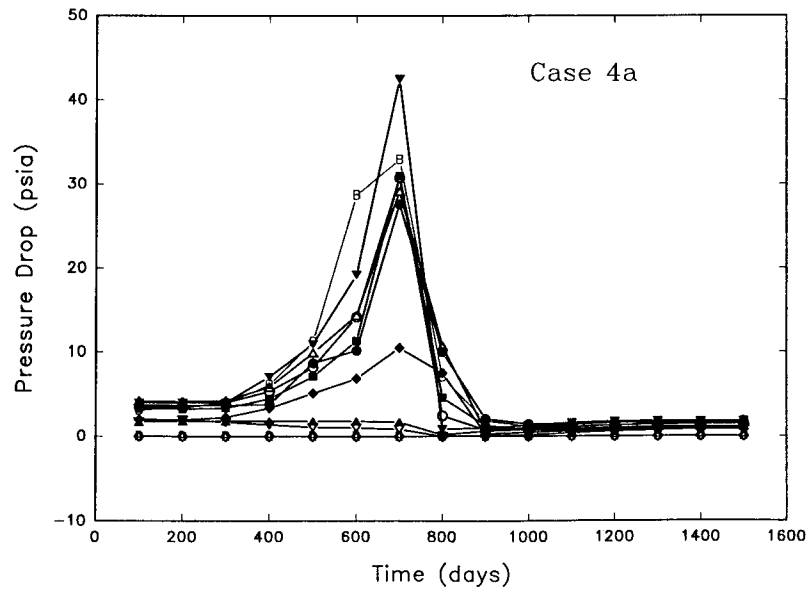


Figure 29: Total pressure drop along wellbore for Case 4a

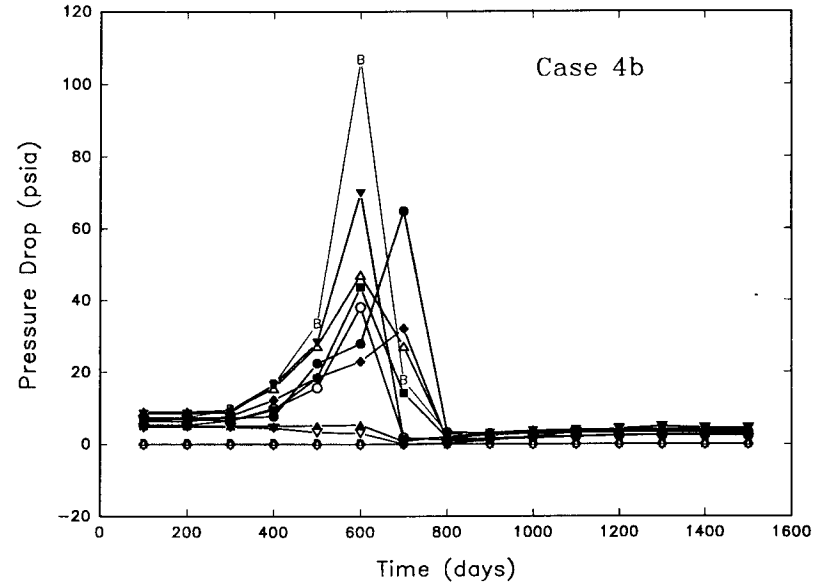


Figure 30: Total pressure drop along wellbore for Case 4b

TIGRESS
Robertson ERC Ltd

ADDENDUM

**Seventh SPE Comparison Solution Project - Modelling Horizontal Wells
in Reservoir Simulation**

Subsequent to our submission of the results of the Seventh Comparative Solution Project, two small errors were discovered in our input data set which significantly affected some of the solutions.

All eight cases have been re-run using the correct data and the results, where they differed from the original ones, can be seen in Figures 3 - 17 and in Tables 8 - 10.

Figure 3: Oil rate (solid) and cumulative oil production (dashed) for Case 1a

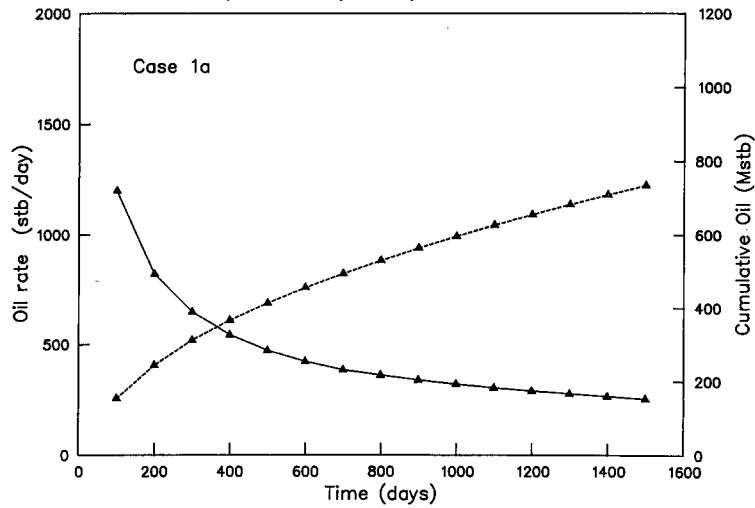


Figure 4: Oil rate (solid) and cumulative oil production (dashed) for Case 1b

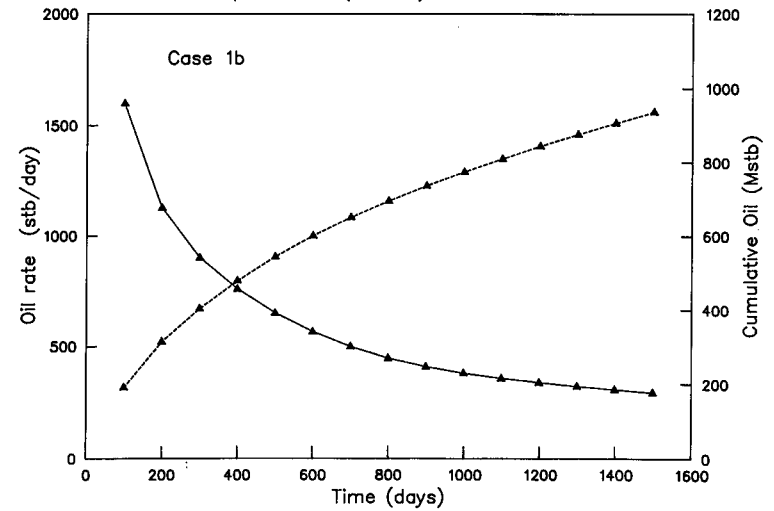


Figure 5: Oil rate (solid) and cumulative oil production (dashed) for Case 2a

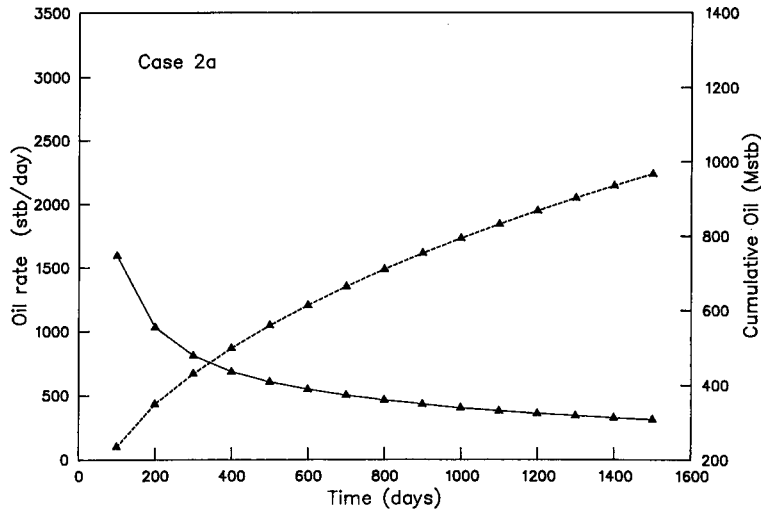


Figure 6: Oil rate (solid) and cumulative oil production (dashed) for Case 2b

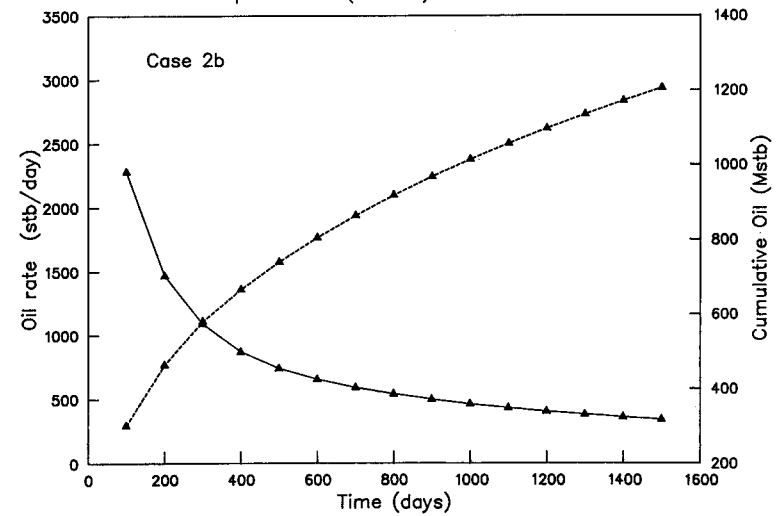


Figure 7: Oil rate (solid) and cumulative oil production (dashed) for Case 3a

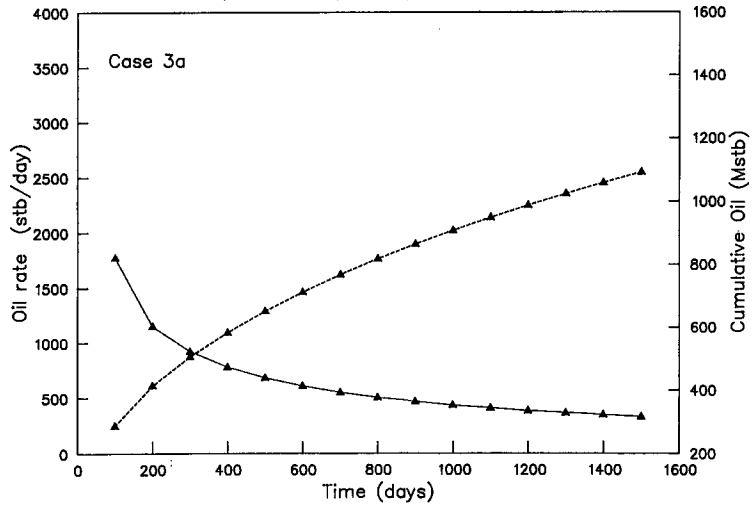


Figure 8: Oil rate (solid) and cumulative oil production (dashed) for Case 3b

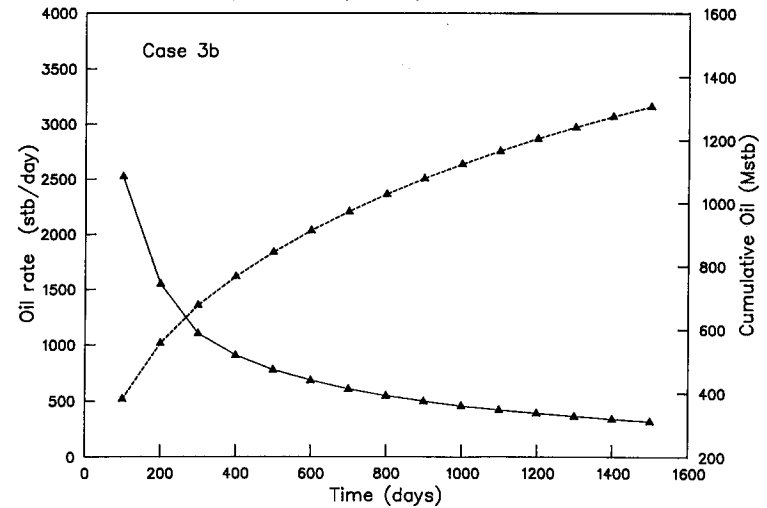


Figure 9: Water-oil ratio for Case 1a

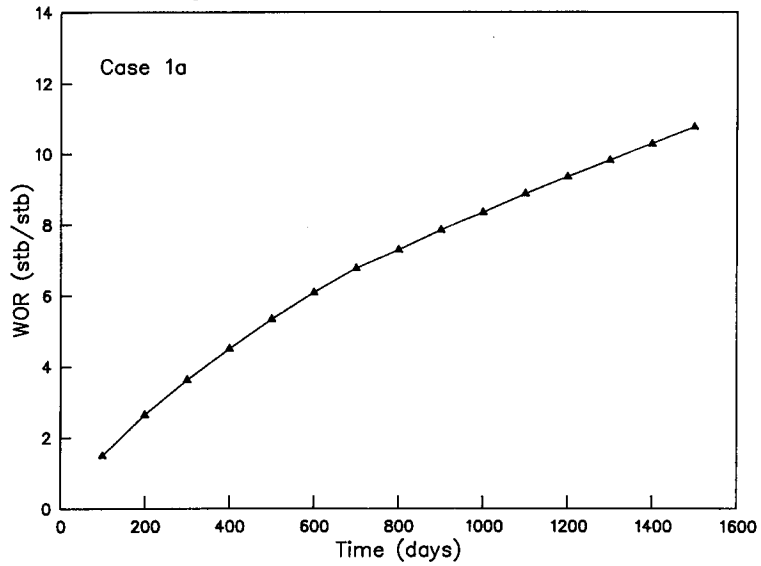


Figure 10: Water-oil ratio for Case 1b

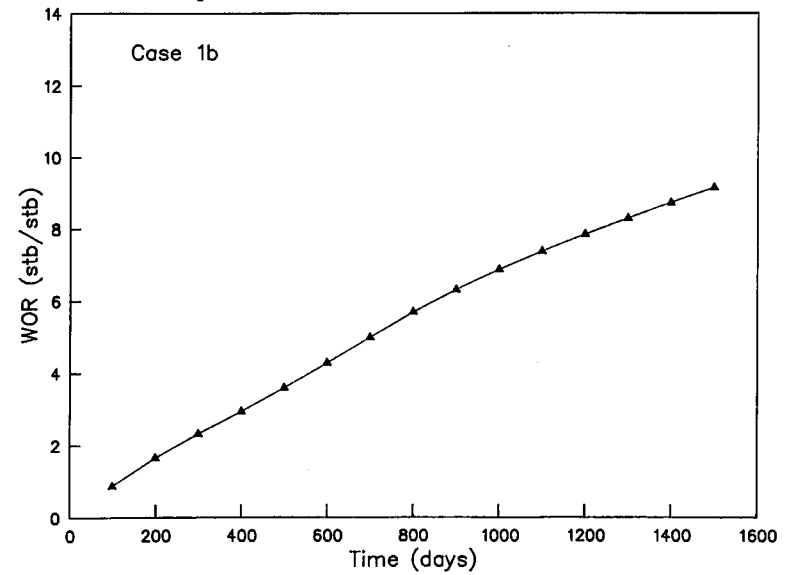


Figure 11: Water-oil ratio for Case 2a

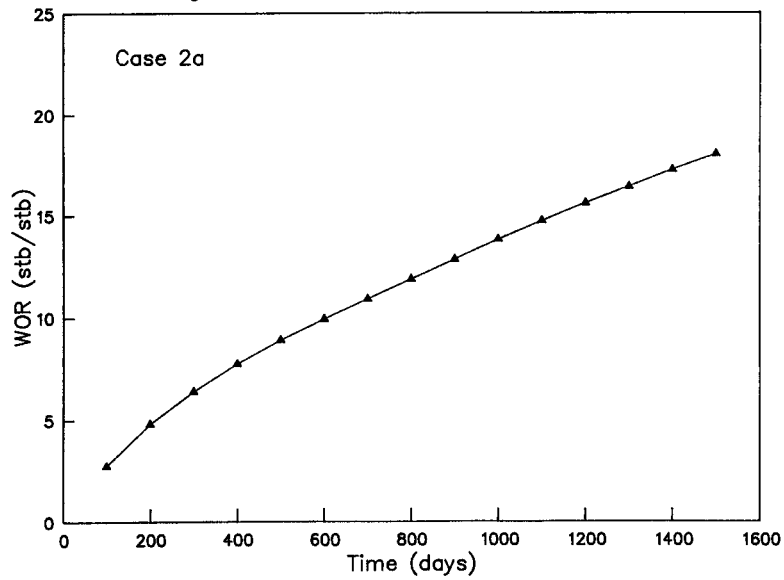


Figure 12: Water-oil ratio for Case 2b

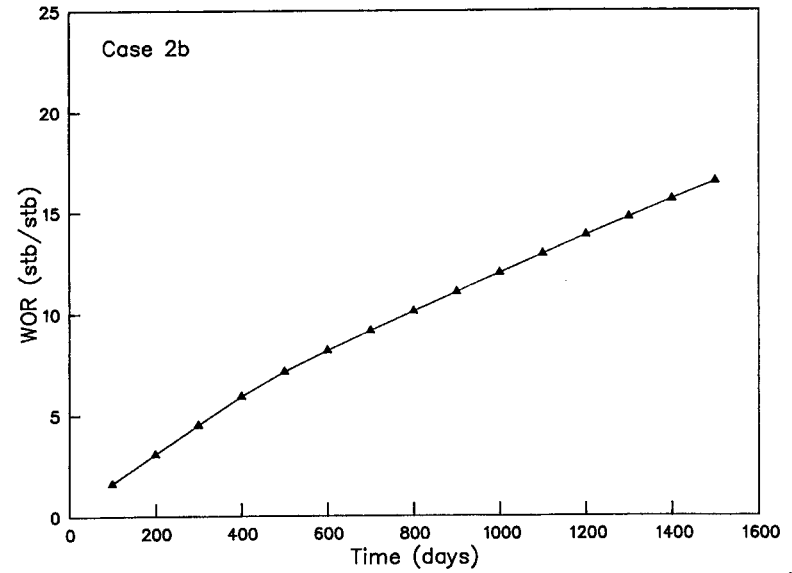


Figure 13: Water-oil ratio for Case 3a

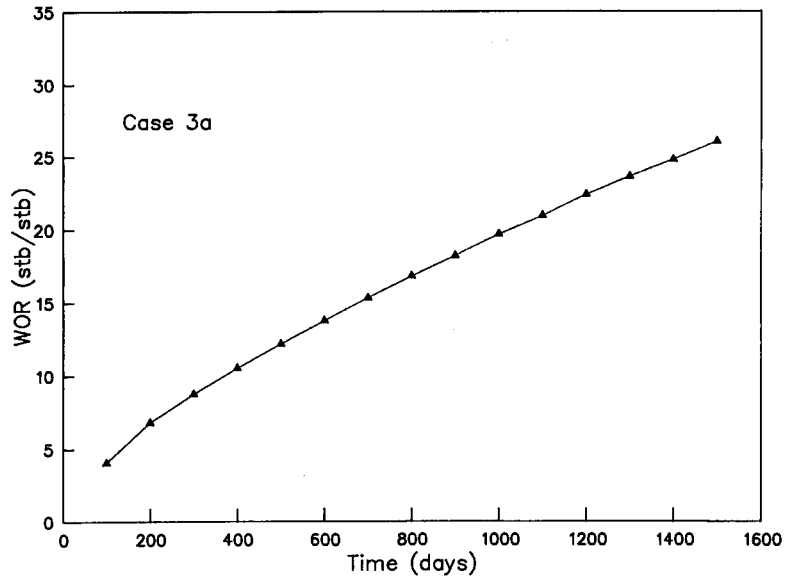


Figure 14: Water-oil ratio for Case 3b

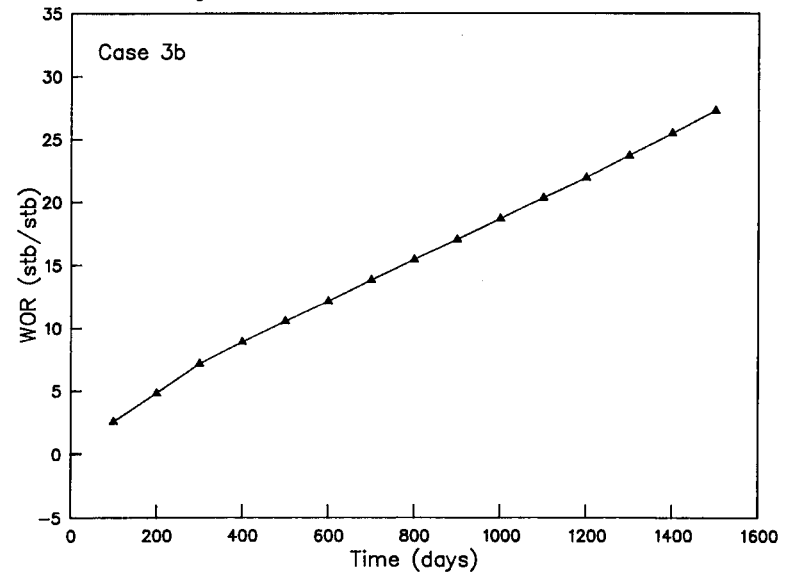


Figure 15: Cumulative water production for Case 1a (solid) and 1b (dashed)

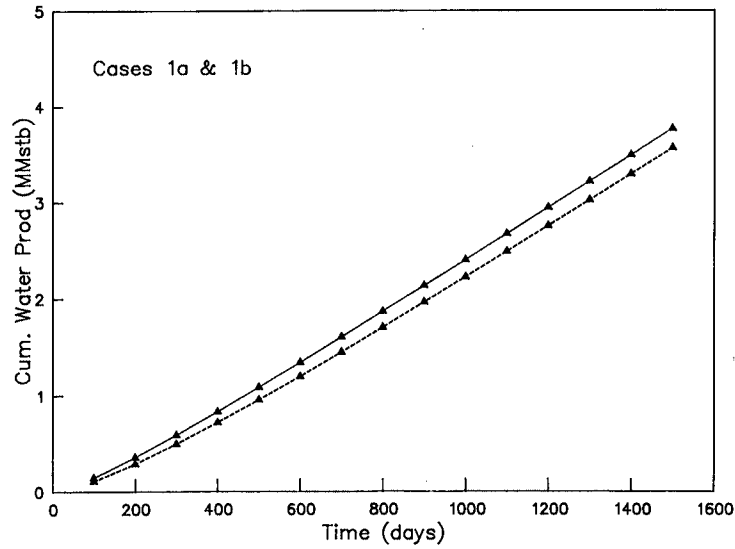


Figure 16: Cumulative water production for Case 2a (solid) and 2b (dashed)

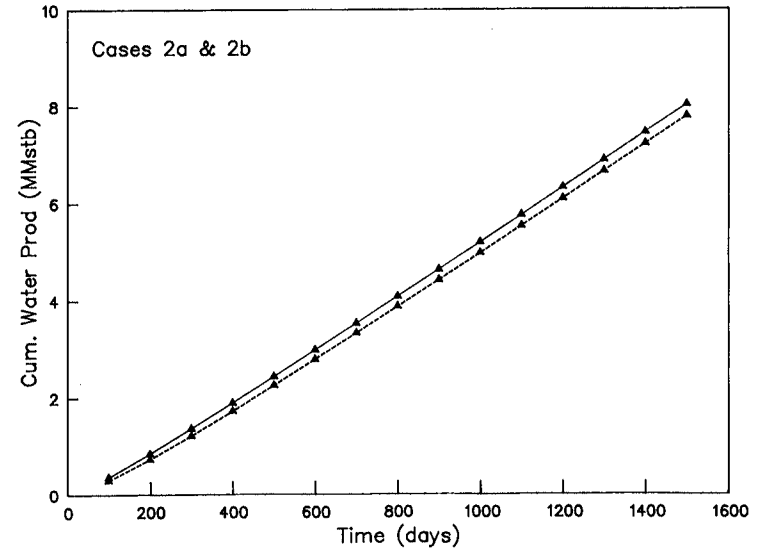


Figure 17: Cumulative water production for Case 3a (solid) and 3b (dashed)

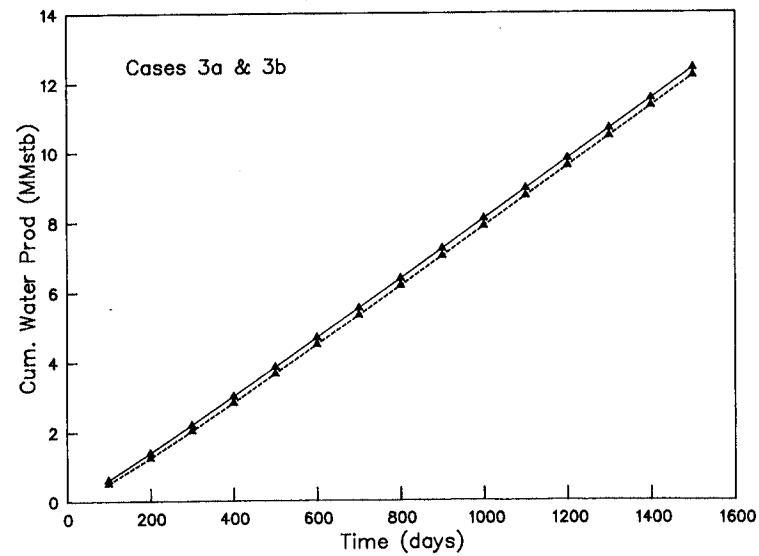


Table 8 Cumulative Oil Production in MSTB at 1500 Days

1a	1b	2a	2b	3a	3b
735.6	936.7	967.0	1206.2	1092.0	1306.8

Table 9 Bottom Hole Pressure in psia at 1500 Days

1a	1b	2a	2b	3a	3b
3444.88	3564.58	3202.85	3457.23	2952.26	3347.14

Table 10 Total Pressure Drop in Wellbore in psia at 1500 Days

1a	1b	2a	2b	3a	3b
0.33	1.05	1.13	3.49	2.25	7.30

ADDENDUM